



10-Hydroxy Decanoic Acid and Zinc Oxide Nanoparticles Retrieve Nrf2/HO-1 and Caspase-3/Bax/Bcl-2 Signaling in Lead-Induced Testicular Toxicity

Adham M. Maher¹ · Ghidaa A. Elsanosy¹ · Doaa A. Ghareeb^{1,2,3} · Samar S. Elblehi⁴ · Samar R. Saleh¹

Received: 28 July 2024 / Accepted: 10 September 2024 / Published online: 30 September 2024
© The Author(s) 2024

Abstract

There has been a significant increase in human exposure to heavy metals (HMs) over the course of the previous century, primarily due to the extensive industrial processes. Male infertility is a prominent complication associated with lead exposure, wherein lead has the potential to accumulate within the testes, resulting in oxidative stress and inflammation. In addition, 10-hydroxydecanoic acid (10-HDA) is a component found in the secretions of worker bees and possesses the capacity to mitigate oxidative stress and prevent inflammation. Due to their advantageous properties, zinc oxide nanoparticles (ZnO-NPs) possess a wide range of applications in the field of biomedicine. This study aimed to assess the therapeutic effect of 10-HDA and ZnO-NPs on testicular toxicity in rats induced by lead acetate (PbAc). PbAc was administered orally for a period of 3 months. Following that, 10-HDA and/or ZnO-NPs were administered for 1 month. PbAc deformed seminal analysis, decreased seminal fructose and sex hormonal levels, and resulted in the development of histopathological complications. Additionally, PbAc increased MDA and decreased Nrf2 and HO-1 expression, confirmed by the declined antioxidant defense system. Furthermore, an increase in testicular inflammatory markers and the Bax/Bcl-2 ratio was observed subsequent to the administration of PbAc. The administration of 10-HDA and ZnO-NPs demonstrated significant efficacy in the restoration of semen quality, pituitary/gonadal hormones, antioxidants, and testicular histoarchitecture. Moreover, 10-HDA and ZnO-NPs decreased testicular inflammatory markers and apoptotic proteins (caspase-3 and Bax expression levels). In conclusion, combining 10-HDA and ZnO-NPs demonstrated synergistic potential in treating PbAc-induced testicular toxicity, thereby presenting a promising approach in nanomedicine and natural drugs.

Keywords 10-HDA · Apoptosis · Bax/Bcl-2 ratio · Inflammation · Male infertility · Oxidative stress · ZnO-NPs

✉ Adham M. Maher
adham.mostafa@alexu.edu.eg

✉ Samar R. Saleh
samar.saleh@alexu.edu.eg; ssaleh84@yahoo.com

Ghidaa A. Elsanosy
ghidaa-atef@alexu.edu.eg

¹ Bio-Screening and Preclinical Trial Lab, Department of Biochemistry, Faculty of Science, Alexandria University, Alexandria 21511, Egypt

² Pharmaceutical and Fermentation Industries Development Centre (PFIDC), The City of Scientific Research and Technological Applications (SRTA-City), Borg Al-Arab, Alexandria, Egypt

³ Research Projects Unit, Pharos University, Alexandria, Egypt

⁴ Department of Pathology, Faculty of Veterinary Medicine, Alexandria University, Alexandria 21944, Egypt

Introduction

Impaired fertility has garnered significant attention as a prominent social concern in developed and industrialized countries [1]. In recent years, there has been a significant increase in the number of infertile couples. Infertility affects approximately 8–17% of couples worldwide. Approximately 50% of cases are caused by male infertility [2, 3]. The characteristic features of male infertility include diminished motility, reduced sperm concentration, and abnormal sperm morphology. Numerous etiological factors contribute to male infertility, including diet, environmental pollutants, exposure to free radicals, and drug treatments [4].

Heavy metals (HMs) refer to a set of naturally occurring metalloids or metals with large densities and atomic weights [5]. HMs naturally exist in the environment in considerable amounts. However, the balance of these metals

in the water and soil was disrupted due to the processes of industrialization and urbanization [6]. HMs can be classified into two categories: essential metals, such as Zn, Co, Cu, Mn, Mg, Se, Cr, Mo, and Fe, and non-essential metals, such as Hg, Cd, and Pb [7]. Essential metals are a class of micronutrients that play a crucial role in biological systems when present in low concentrations. However, their detrimental effects become apparent when they exceed a specific threshold. In contrast, non-essential metals lack biological value and exhibit toxicity even at minimal concentrations. When the HMs intake rate exceeds the excretion rate, HMs tend to accumulate within tissues [8]. The ability of these elements to accumulate in living organisms and their non-biodegradable properties has demonstrated their potential to induce detrimental effects on specific organs, thereby capturing the interest of researchers in the field of heavy metal toxicity. The extent of heavy metal toxicity is influenced by various factors, including the dose, modality, and duration of exposure, as well as gender, genetics, age, and nutritional status [6]. The detrimental effects of non-essential heavy metals (HMs) stem from their capacity to modify the antioxidant system, generate reactive oxygen species (ROS), interact with and break down DNA, bind to unbound sulfhydryl groups, and displace binding sites on a vast array of enzymes, receptors, and transport proteins. Therefore, a multitude of adverse effects on biological systems are manifested. For instance, disorders such as compromised immune system function, metabolic impairment, imbalanced hormone levels, organ dysfunction, congenital abnormalities, and malignancy were documented [9–11].

Lead (Pb) is widely recognized as one of the most abundant toxic heavy metals found in the environment [12]. Due to the Industrial Revolution, substantial amounts of this metal inhabited the air, water, and soil, causing severe health problems to all living organisms [12]. Current sources of lead toxicity include water pipes, pesticides, batteries, cables, and gasoline additives [13]. The toxicity of lead is attributed to its extended biological half-life, which enables its accumulation in various organs such as the bone, liver, kidneys, brain, and testes. This accumulation results in a diverse array of physiological and biochemical changes, ultimately leading to conditions such as anemia, renal failure, neurological dysfunctions, impaired fertility, and eventually death [6, 14, 15]. Lead can introduce toxicity by increasing the generation of ROS while impairing the antioxidant defense system, causing oxidative stress. Furthermore, lead can disrupt testosterone production and harm cells involved in the development of sperm, such as Sertoli cells, Leydig cells, and Spermatogonia cells, causing infertility and decreased sex drive [12, 16]. Markets are flooded with synthetic products to deal with infertility problems, accompanied by uncertain results and serious side effects. Common contemporary therapeutic interventions encompass

antibiotics, antiphlogistics, kallikrein, corticosteroids, and hormone preparations [11, 17, 18].

Natural products have long been regarded as therapeutic agents in the field of folk medicine due to their significant efficacy in promoting human health. Many of these natural products are dispersed in the pharmaceutical market owing to their defensive role against the damaging effects of oxidative stress, inflammation, and drug side effects. Bioactive compounds, whether in isolation or in combination, can be employed as natural products to exert beneficial effects on the male reproductive system [19]. Bee-derived products possess a high concentration of bioactive compounds, rendering them suitable for incorporation into complementary medication, such as treating male reproductive impairment [20]. Royal Jelly (RJ) is produced by nurse bees and secreted from their mandibular and hypopharyngeal glands. In addition, it serves as the sole dietary source for adult queens throughout their lifespan [21–23]. The saturated hydroxyl fatty acid known as 10-hydroxydecanoic acid (10-HDA) is widely recognized as one of the primary fatty acids present in propolis, honey, and RJ [24–29]. The majority of RJ fatty acids are diacids or hydroxyls. The hydroxyl and carboxyl groups located at the head and tail of the carbon chain possess the ability to facilitate the removal of molecular oxygen and the capture of reactive oxygen species that are detrimental to biological processes. These functional groups contribute to the manifestation of biological activities such as antioxidant and anti-inflammatory properties [28]. 10-HDA has a variety of unique physiological activities, including immune-regulating, glucose-regulating activity, anticancer, bactericidal, antioxidant, and anti-inflammatory properties [27, 29–31].

Nanoparticles (NPs) are miniature particles with a size below 100 nm. The significance of particles at the nanoscale was first recognized by scientists when they observed that the size of a substance can influence its properties [32]. Additionally, the modification of the physical, optical, and surface properties of NPs has provided them with a diverse array of potential applications, including their use in medicinal applications for diagnosis, imaging, and therapy [33]. Recently, the beneficial effects of zinc oxide nanoparticles (ZnO-NPs) have facilitated their extensive utilization in various biological and animal scientific contexts due to their outstanding characteristics of solubility, compatibility with biological systems, low price, and minimal toxicity. The topographies of ZnO-NPs allow them to simulate biomolecules that facilitate the regulation of cellular homeostasis through their antioxidant properties [34–36]. Therefore, ZnO-NPs have garnered significant interest across various biomedical fields due to their antidiabetic, antibacterial, anticancer, antioxidant, and anti-inflammatory activities [37]. Furthermore, the detoxifying potential of ZnO-NPs against heavy metal toxicity has been previously examined.

Specifically to heavy metals, these particles demonstrated the ability to alleviate allergic dermatitis in rats that were induced with lead oxide [38]. Also, the administration of ZnO-NPs has been shown to mitigate CdCl₂-induced tongue toxicity in albino rats [39].

The pharmacological activity of 10-HDA, the second most abundant fatty acid in RJ, has been the subject of limited studies, primarily focusing on cellular mechanisms [22]. Therefore, the rationale for conducting this study was based on the scarcity of research regarding the antioxidant and anti-inflammatory characteristics of 10-HDA in alleviating testicular damage resulting from lead exposure, as well as its potential synergistic effects when combined with ZnO-NPs. The primary aim of this study was to assess the efficacy of these interventions in ameliorating lead-induced testicular damage by examining various markers related to antioxidant activity, anti-inflammatory, and anti-apoptotic pathways.

Material and Methods

Chemicals

Trichloroacetic acid (TCA, Cat. No. T6399), Tris-HCl (Cat. No. T15760), 5,5'-dithiobis(2-nitrobenzoic acid) (DTNB, Cat. No. D8130), reduced glutathione (GSH, Cat. No. G4251), sulfosalicylic acid dihydrate (Cat. No. S2130), and 10-HDA (99% purity, Cat. No. 379700) were obtained from Sigma-Aldrich, St. Louis, USA. Zinc oxide nanoparticles (ZnO-NPs, 30–50 nm, purity 99.9%, Cat. No. NRL03041) were obtained from Nano Research Lab, Jamshedpur, India. Lead (II) acetate trihydrate (Pb(CH₃COO)₂·3H₂O, PbAc) was purchased from Alpha Chemika Co. Andheri, west-Mumbai, India (Cat. No. AL2686). A specific seminal fructose kit was purchased from Spectrum Diagnostics, Egypt (Cat. No. FR2310). GENEzol™ Reagent was purchased from Geneaid, Taiwan (Cat. No. GZR100). TOPscript™ RT DryMIX (dT18/dN6) and TOPreal™ qP CR 2X PreMIX (SYBR Green with low ROX) were obtained from Enzynomics, Korea (Cat. Nos. RT220 and RT500M, respectively). Primers were obtained from Willowfort, UK. Roche Elecsys testosterone II (Cat. No. 05200067190), Roche Elecsys luteinizing hormone (LH, Cat. No. 11732234122), and Roche Elecsys follicle-stimulating hormone (FSH, Cat. No. 11775863122) kits were purchased from Roche Diagnostics, Indianapolis, IN. All chemicals used were of high analytical degree.

Characterization of Zinc Oxide Nanoparticles

Zinc oxide powder was suspended in 10 ml of ethanol and left for 1 h in an ultrasonic cleaner [40]. Subsequently, a copper grid coated with a Formvar membrane was loaded with 4 μl

of the ZnO-NPs sample [41]. The grid was subsequently put inside the JEOL-JSM-1400 PLUS (TEM) transmission electron microscope's sample holder, and the sample was examined [42].

Scanning Electron Microscopy (SEM) (JEOL JSM-IT 200) equipment was used to determine the optical properties and nanostructure morphology of ZnO-NPs. Therefore, the solid was coated with a thin conductive gold coating on a double-sided carbon tape, followed by subsequent analysis [43]. The element composition of the samples and the purity of ZnO-NPs were determined using energy-dispersive X-ray spectroscopy (EDX) (JOEL-IT 200) [41, 44].

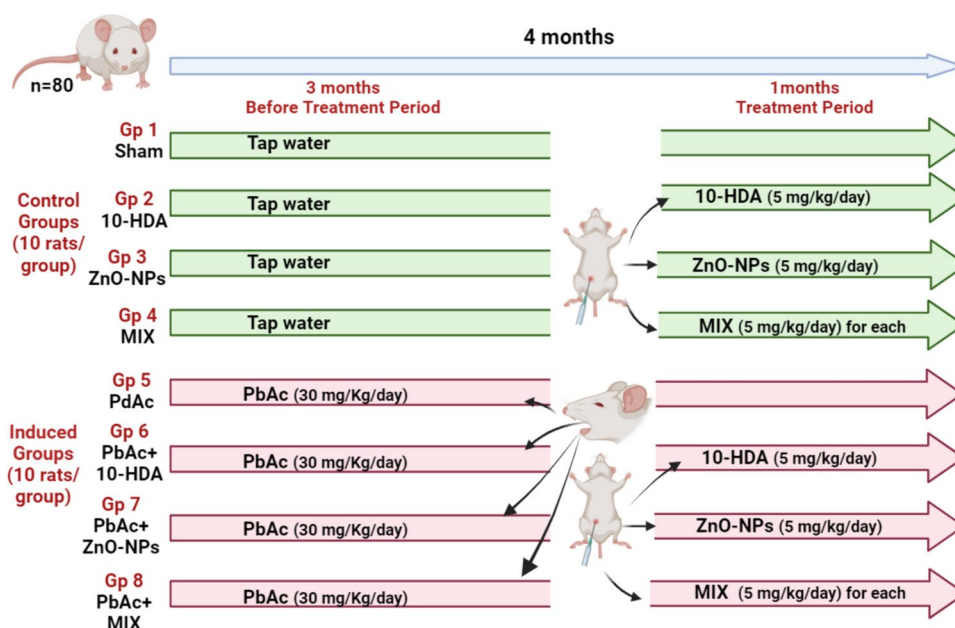
Animals and Experimental Design

The present study utilized a sample of 80 mature male Sprague Dawley rats weighing between 150 and 200 g and aged 10–12 weeks. The animals were obtained from the Institute of Graduate Studies and Research's animal house at Alexandria University, Egypt. All animal procedures adhered to the ARRIVE guidelines. All animal treatments were conducted in accordance with the ethical guidelines for scientific research established by the Institutional Animal Care and Use Committee (IACUC) of Alexandria University (AU: 04 22 10 22 1 01). The animals were housed in polypropylene cages (5 rats/cage) in a well-ventilated room in a regulated setting for a 12:12-h diurnal period. Rats had unrestricted access to food (growing fodder 21% protein, Elfagr Company, Egypt) and water. Following a week of acclimation, rats were randomly divided into eight groups (10 animals/group), as shown in Fig. 1. The control groups included (1) sham group, (2) 10-HDA group, (3) ZnO-NPs group, (4) mix group (mixture = 10-HAD + ZnO-NPs). The infertility-induced groups included (1) PbAc group, (2) PbAc + 10-HDA group, (3) PbAc + ZnO-NPs group, and (4) PbAc + mix group (mixture = 10-HAD + ZnO-NPs). Lead-induced infertility was achieved using oral gavage of PbAc (30 mg/kg/day) for 3 months [45, 46]. Doses were calculated and prepared weekly in correspondence with the body weight of each rat. Pb-acetate was formulated via dissolution in distilled water. Following the Pb-acetate induction, a treatment scheme was initiated by the administration of 10-HDA (5 mg/kg body weight) [47] and/or ZnO-NPs (5 mg/kg body weight) [48–50]. The doses were prepared by dissolving the corresponding doses in Polly ethylene glycol, taking into consideration the body weight of each rat. Treatments were administered intraperitoneally on a daily basis at a consistent time each day for a duration of 4 weeks.

Collecting and Handling Blood and Testicular Tissues

Following the conclusion of the experimental period, the rats were fasted overnight and then were anesthetized with

Fig. 1 Experimental design and group classification



isoflurane inhalation (4% for 2–3 min) in preparation for decapitation [51]. Blood samples were collected from the inferior vena cava, followed by centrifugation to obtain the sera, and stored at -20°C . For biochemical and molecular evaluations, the left testes were stored at a temperature of -80°C . The testicular tissue was homogenized in Tris HCl buffer (20 mM, pH 7.4) at a 1:9 (w/v) ratio. This resulted in the formation of a supernatant, which was subsequently stored at -80°C for the purpose of analyzing fructose levels, inflammation markers, apoptotic markers, and biomarkers associated with oxidative stress. Histopathological examination was conducted on the right testicles of each animal using 10% neutral formalin fixation. The epididymis was isolated for seminal analysis.

Epididymis Seminal Quality and Seminal Fructose Level

The epididymis was carefully divided using scissors to release the spermatozoa into a clean petri dish. The dish contained 2 ml of Ham's F-10 and 0.5% bovine serum albumin (BSA). A comprehensive assessment of the epididymis sperm count, morphological index, and motility was conducted using a hemocytometer. All equipment and materials were preheated and kept at 37°C . In order to ensure accuracy, four counts were conducted on each sample, and the average was calculated [52, 53].

Seminal fructose level was measured using the spectrophotometric method according to a previous study [54]. A homogeneous mixture consisting of 500 μl TCA (1 mol/l) combined with either standard fructose (300 mg/dl), supernatant of testis homogenate, or distilled water (blank) was

prepared. After 10 min at ambient temperature, the mixture was centrifuged for 10 min at 3000 rpm. Subsequently, 1 ml of hydrochloric acid (9 mol/l) and 50 μl of resorcinol (9 mmol/l) were combined with the supernatant, mixed, and then set for 5 min in a bath of boiling water. The produced color was measured in relation to the blank at 495 nm. The analysis of fructose levels in testicular tissue was conducted and expressed as mg/g.

Determination of Testicular Lead Content

Wet digestion was utilized to determine the Pb content in the testes. First, 300 mg of the testes tissue was dehydrated at 120°C overnight in an oven. Then, the dried sample was carefully placed in a cold muffle furnace and subjected to a gradual temperature increase. The temperature rose from ambient to 450°C at a constant rate of 50°C per hour. Subsequently, the sample was subjected to digestion using concentrated nitric acid and further dried in the muffle at 450°C for 1 h. The resulting powder was dissolved in 1 N hydrochloric acid and then appropriately diluted using 0.2% nitric acid. Lead concentration in the testicular sample was detected utilizing flame atomic absorption spectrophotometry, specifically employing the Shimadzu model (AA-6650). The absorbance was measured at 283.3 nm, following the protocol defined by Szkoda and Zmudzki [55].

Serum Pituitary/Gonadal Hormones

The measurement of serum luteinizing hormone (LH), follicle-stimulating hormone (FSH), and testosterone levels was conducted in accordance with the manufacturer's

instructions of the ELISA kits (COBAS, Indianapolis, IN 46256, USA). An ELISA reader (ELx800, Bio-TEK, Winooski, VT, USA) was used to measure the absorbance at 450 nm. LH and FSH levels were reported as $\mu\text{U/ml}$, whereas testosterone was expressed as ng/dl .

Testicular Oxidative Stress Markers

The frozen testicular tissues were homogenized in a solution containing a protease inhibitor and lysis buffer (1% Triton X-100, 150 mM NaCl, 10 mM Tris, pH 7.4), then centrifuged for 10 min at 4 °C at 10,000 g. Following that, the supernatant was collected. Malondialdehyde (MDA) level was assessed as a marker of lipid peroxidation. Under acidic conditions, MDA combines with thiobarbituric acid (TBA) to generate a pink product that, when heated, can be detected spectrophotometrically at 532 nm. The amount of MDA in the testicles was reported as $\mu\text{mol/mg}$ protein [56]. Testicular nitric oxide (NO) content was measured spectrophotometrically following the method by Montgomery and Dymock [57]. The application of a diazotizing agent, such as sulfanilamide, in an acidic environment to nitrite resulted in the formation of an intermediate diazonium salt. This salt subsequently reacts with N-naphthyl-ethylenediamine, forming a stable azo compound. The resulting deep purple hue was measured at 540 nm and stated as mM/mg protein. Reduced glutathione (GSH) was measured using Ellman's method [58]. GSH reacts with 5,5'-dithio-bis-2-nitrobenzoic acid (DTNB), creating a 2-nitro-5-thiobenzoic acid product. The yellow-colored product was detected at 412 nm and represented as $\mu\text{mol/mg}$ protein [59]. The assessment of glutathione-S-transferase (GST) activities in the testicles was conducted following the protocol outlined by Habig [60]. GST catalyzes the reaction between GSH and p-nitrobenzyl chloride, forming glutathione nitrobenzyl, which was detected at 310 nm and quantified as U/mg protein. For superoxide dismutase (SOD), the inhibitory effect of SOD on the pyrogallol autooxidation was assessed spectrophotometrically at 420 nm. The amount of enzyme required to decrease pyrogallol autooxidation by 50% is equivalent to one unit of SOD activity. The SOD activity was reported as U/mg protein [61].

For the estimation of enzymes' specific activity (U/mg protein), the total testicular protein was measured, with BSA (1 mg/ml) serving as a reference in accordance with the Lowry method [62].

Quantitative Real-Time Reverse Transcription PCR Analysis (qRT-PCR)

The extraction of total RNA (50–100 mg) from testicular tissue was conducted in accordance with the manufacturer's instructions, utilizing GENEzol™ Reagent. For estimating

the concentration and purity of the isolated RNA, a NanoDrop 2000 spectrophotometer (Thermo Scientific, USA) was used to measure the absorbance at 260 nm and 280 nm (A260/280). Samples with A260/280 ≥ 1.8 were considered for further analysis. Using TOPscript™ RT DryMIX (dT18/dN6) and 5 μg of the extracted RNA, cDNA synthesis was carried out. For qRT-PCR analysis, 1 μl cDNA was mixed with 1 μl forward primer, 1 μl reverse primer, 10 μl TOPreal™ qPCR 2X PreMIX (SYBR Green with low ROX), and RNase-free water to reach a final volume of 20 μl per well. To perform quantitative PCR, the CFX96™ Real-Time System was utilized (BIO-RAD, USA) with the following thermal protocol: initial denaturation lasting 12 min at 95 °C, then 45 cycles of denaturation for 10 s at 95 °C, annealing for 30 s at 52 °C, and extension for 30 s at 72 °C. Duplicate samples were loaded for each analysis. The comparative $2^{-\Delta\Delta\text{CT}}$ method was exploited to determine the fold change in the target gene compared to the sham control calibrator. The GAPDH mRNA level was used to normalize the data. The targeted genes' primer sequences for glyceraldehyde phosphate dehydrogenase (GAPDH, NM_017008.4), tumor necrosis factor- α (TNF- α , NM_012675.3), interleukin-1 β (IL-1 β , NM_031512.2), IL-6 (NM_031168.1), IL-8 (NM_017183.2), B-cell lymphoma 2 (Bcl-2, NM_016993.2), Bcl-2 Associated X-protein (Bax, NM_017059.2), and cysteine-aspartic acid protease (caspase-3, NM_012922.2) are adopted from [63], as depicted in Table 1.

Western Blotting Analysis

Testes tissue protein extract was used to examine the levels of protein expression for nuclear factor erythroid 2-related factor-2 (Nrf2), heme oxygenase-1 (HO-1), and inhibitor of nuclear factor $\kappa\beta$ kinase (Phospho-IKK α/β). This was done following the established protocol outlined by Mahmood and Yang (2012). Specific antibodies were utilized, including rabbit monoclonal antibodies for HO-1, Phospho-IKK α/β , and Nrf2 (designated as #2697 s, #82206 s, and #20733, respectively, from Cell Signaling Technology, USA). Additionally, a rabbit monoclonal antibody β -actin 13E5 (#4970, Cell Signaling Technology, USA) and goat anti-rabbit IgG, AP-linked Ab (#7054, Cell Signaling Technology, USA) were utilized. In order to visualize the protein bands, NBT/BCIP solution (Thermo Fisher Scientific, USA) was utilized, obeying the instructions provided by the manufacturer. The protein bands' intensity was quantified using Quantity One software (Bio-Rad Laboratories, USA). For accurate comparison, the intensity of the protein bands was normalized to β -actin. The results were then reported as a relative intensity normalized to β -actin, facilitating interpretation and analysis.

Table 1 Primer sequences of genes analyzed in real-time PCR

Gene name	Primer sequence	
GAPDH	F 5'-AGATCCACAACGGATACATT- 3'	R 5'-TCCCTCAAGATTGTCAGCAA- 3'
TNF- α	F 5'-ACACACGAGACGCTGAAGTA- 3'	R 5'-GGAACAGTCTGGGAAGCTCT- 3'
IL-1 β	F 5'-GACTTCACCATGGAACCCGT- 3'	R 5'-GGAGACTGCCCATCTCGAC- 3'
IL-6	F 5'-GCCAGAGTCATTGAGCAATA -3'	R 5'-GTTGGATGGTCTTGGTCCTTAG-3'
IL-8	F 5'-CATTAATATTTAACGATGTGGATGCG-3'	R 5'-GCCTACCATCTTTAAACTGCACAAT-3'
Bcl-2	F 5'-GCAGTCTCTTCCCGGAAGGA-3'	R 5'-AGGTGCAGCTGACTGGACATCT-3'
Bax	F 5'-AACTTCAACTGGGGCCGCGTGGTT-3'	R 5'-CATCTCTTCCAGATGGTGAGCGAG-3'
Caspase-3	F 5'-GTGGAAGTACGATGATATGGC-3'	R 5'-CGCAAAGTACTGGATGAACC-3'

GAPDH, glyceraldehyde-3-phosphate dehydrogenase; *TNF- α* , tumor necrosis factor-alpha; *IL-1 β* , interleukin-1beta; *IL-6*, interleukin-6; *IL-8*, interleukin-8; *Bcl-2*, B-cell lymphoma 2; *Bax*, Bcl-2 Associated X-protein; *Caspase-3*, Caspase 3

Combination Index Analysis

The quantitative assessment of the combined effects of ZnO-NPs and 10-HDA was done by calculating the combination index (CI). The combination therapy has the potential to yield synergistic (when $CI < 1$), antagonistic (when $CI > 1$), or additive (when $CI = 1$) outcomes compared to using each treatment separately. The determination of the combination index was conducted following the methodology described by Zhou [64] and Saleh [2]. For the computation of the combination index, the predictive value for the combination of 10-HDA/ZnO-NPs was initially determined using the following equation:

$$\text{The Predicted value} = \left(\frac{\text{Observed value for 10 - HDA}}{\text{Control value}} + \frac{\text{Observed value for ZnO - NPs}}{\text{Control value}} \right) \times \text{Control value}$$

The CI was calculated using the formula:

$$CI = \frac{\text{Observed value}}{\text{Predicted value of the combination}}$$

Testicular Histopathological Examination

Testicular tissue specimens were immediately preserved in phosphate-buffered formalin (10%, pH 7.4) after necropsy and left for at least 24 h prior to undergoing treatment using the standard paraffin embedding method [65]. Five micrometer-thick sections were cut, placed on xylene-deparaffinized slides, and rehydrated with ethanol at progressively decreasing concentrations. Hematoxylin and eosin (H&E) staining was applied to slides for routine histopathological settings. A Leica DM500 light microscope was used for a blind analysis of stained sections, and a digital camera was used to take

pictures of the sections at a magnification of 100 (EC3, Leica, Germany). A histological lesion-scoring system was used to indicate the severity of histopathological lesions. Within each animal group, a total of ten slides stained with H&E were examined. Each slide was assigned to a specific rat, and the pathological lesions were assessed using a blind method. The grading process involved evaluating ten random fields per slide, which included degenerated germinal epithelial cells, buckled basement membrane, sloughed degenerated germinal epithelial cells, intertubular vascular congestion, and interstitial edema. The intensity of pathological lesions was determined by assessing the percentage of damaged tissue across

the entire section. Based on the percentage of damaged tissue throughout the entire section, the intensity of pathological lesions was expressed as None (0): normal histology with no impact from the field under investigation, Mild (1): 5–25% of the scanned field was implicated, Moderate (2): 26–50% of the field under investigation was affected, Severe (3): 50% engagement in the field under examination. In order to determine the overall tissue damage scores, the scores for each parameter were aggregated [66].

Statistical Analysis

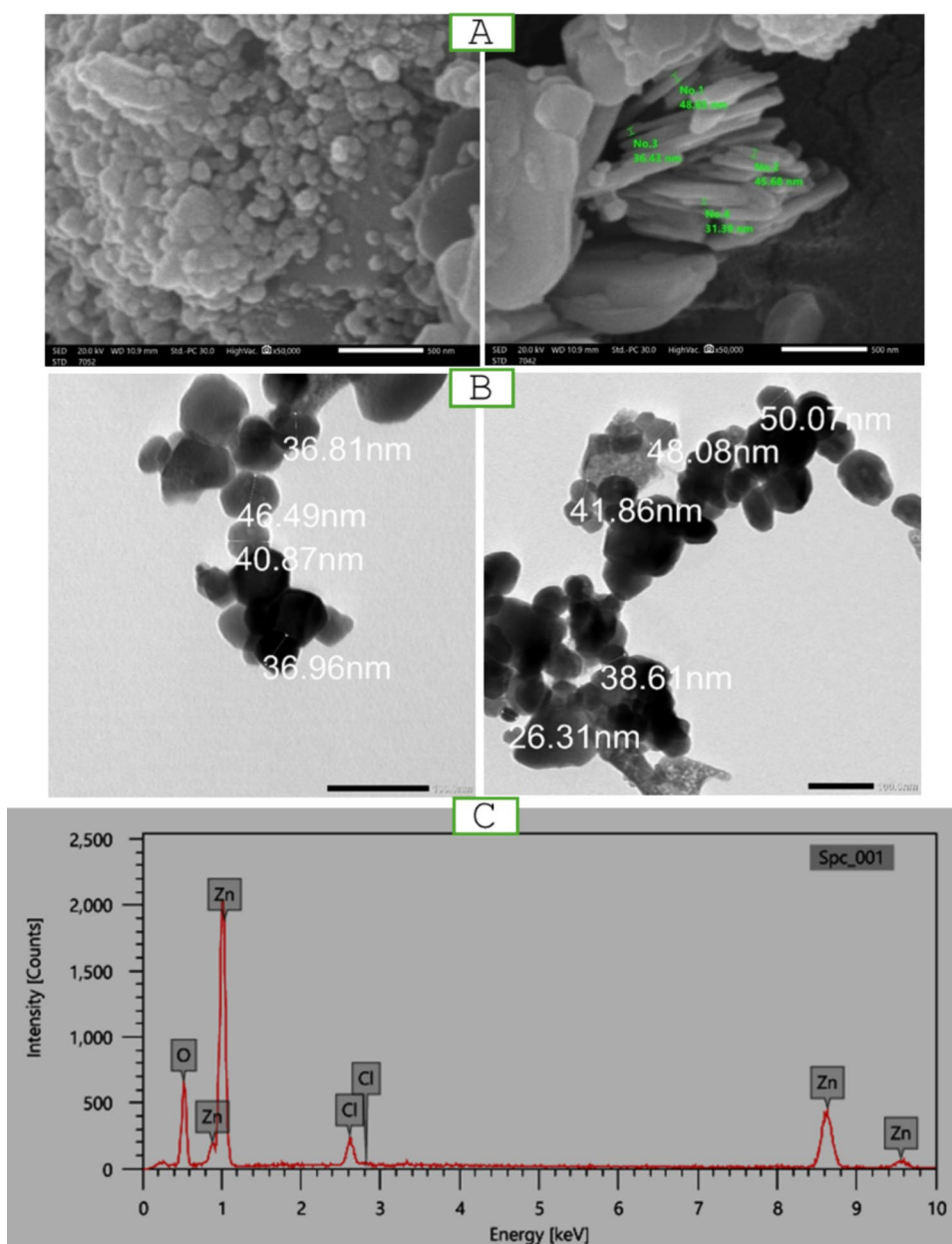
The SPSS software, version 16.0 (Chicago, IL, USA), was used for statistical tests, and the results were expressed as the mean \pm SD. Using the LSD test and one-way ANOVA, differences within groups were statistically analyzed. In addition, a p -value of < 0.05 was considered statistically significant.

Results

Characterization of ZnO-NPs

The SEM micrograph of ZnO-NPs shows a spherical homogeneous shape of the nanoparticles, whereas the average particle size for the nanoparticle is about 50 nm (Fig. 2A). The microscopic image from TEM revealed a hexagonal shape for ZnO-NPs (Fig. 2B). The EDX data revealed the presence of two elements: Zn (70.08%) and O (24.60%) and a neglectable amount of Cl (5.31%), thus confirming the high purity of ZnO-NPs, as depicted in (Fig. 2C).

Fig. 2 Characterization of ZnO-NPs. (A) SEM micrograph of ZnO-NPs in scale bar 500 nm. (B) TEM micrograph of ZnO-NPs. (C) EDX data of ZnO-NPs



The Impact of Lead Acetate Exposure and Different Treatments on Seminal Analysis and Seminal Fructose Level Among the Investigated Groups

Figure 3A shows normal sperm morphology of sham, 10-HDA, ZnO-NPs, and MIX groups. Conversely, animals exposed to PbAc exhibited anomalous sperm morphology characterized by head and tail abnormalities, specifically round heads and coiled tails. Additionally, detachments were observed in these animals. In contrast, the application of 10-HDA and/or ZnO-NPs treatments resulted in enhanced sperm morphology. Table 2 illustrates that the group exposed to PbAc exhibited a statistically significant decrease ($p < 0.05$) in the number of sperm in the epididymis, as well

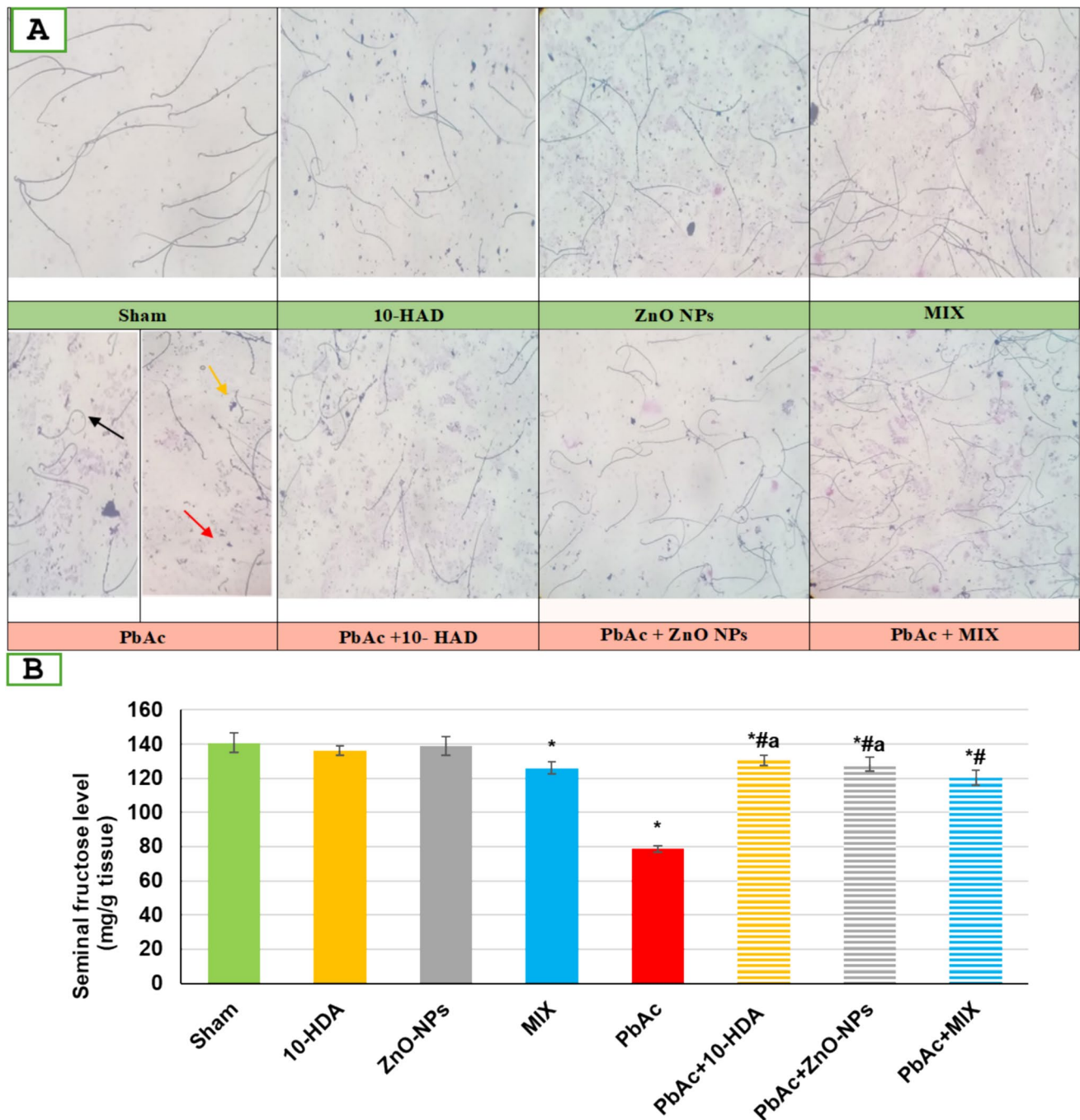


Fig. 3 The impact of lead acetate exposure and different treatments on seminal analysis (A) and fructose level (B) in different experimental groups. Sperm morphology was stained using the Diff-Quick procedure. Sham and treated controls (10-HDA, ZnO-NP, and MIX groups) show normal sperm morphology of heads and tails. The

PbAc-induced group exhibited sperm abnormalities as coiled tail (black arrow), detached head (red arrow), and detached tail (yellow arrow). PbAc + 10-HDA, PbAc + ZnO-NP, and PbAc + MIX treatments resulted in the restoration of normal sperm morphology (A)

as a reduction in the morphology index, sperm progressive motility, and percentage of motility during the first, second, and third hour. Furthermore, there was a notable increase in non-progressive motility compared to the control group. In contrast, the lead-induced rats receiving treatments revealed

significant ($p < 0.05$) recovered semen quality as related to the PbAc untreated group. Regarding seminal fructose levels (Fig. 3B), PbAc-induced infertility rats showed a significant ($p < 0.05$) decline in seminal fructose levels compared to the sham group. However, administering 10-HDA and/

Table 2 The impact of lead acetate exposure and different treatments on seminal analysis including sperm count, morphology index, motility type, and motility time

Parameters	Sham	10-HAD	ZnO-NPs	MIX	PbAc	PbAc + 10-HDA	PbAc + ZnO-NPs	PbAc + MIX	
Sperm count (10 ⁶ /ml)	206 ± 4.55	192.8 ± 1.71*	194.75 ± 0.96*	203.5 ± 4.065	152.25 ± 5.74*	168.5 ± 1.29* ^{#a}	191 ± 0.58* ^{#a}	198.5 ± 1.83* [#]	
Morphology index (%)	80.5 ± 1.29	78.8 ± 4.11	79.25 ± 0.96	82.5 ± 1.29	72.5 ± 1.29*	77.5 ± 1.29* [#]	80.0 ± 0.82 [#]	79.5 ± 1.29 [#]	
Motility type (%)	Progressive	59.75 ± 1.71	57.5 ± 1.29	58.5 ± 1.29	56.5 ± 2.08*	49.25 ± 1.71*	52.0 ± 2.16* ^a	53.5 ± 1.29*	55.5 ± 0.58*
	Non-progressive	10.75 ± 2.63	11.5 ± 1.29	11.5 ± 1.29	9.75 ± 0.96	21.5 ± 2.38*	10.0 ± 2.16* ^{#a}	8.5 ± 2.38 [#]	8.5 ± 1.29 [#]
Motility (%)	1st h	62.25 ± 1.71	64.5 ± 1.29	57.5 ± 1.29*	69.5 ± 1.29*	49.5 ± 1.29*	64.0 ± 2.94* ^a	60.5 ± 1.29* ^a	71.25 ± 2.22* [#]
	2nd h	40.5 ± 1.29	38 ± 0.82*	34.5 ± 1.29*	43 ± 2.16*	28.5 ± 1.29*	39.8 ± 1.71* ^{#a}	35.8 ± 2.75* ^{#a}	46.5 ± 1.29* [#]
	3rd h	11.25 ± 1.71	9.5 ± 2.38	8.5 ± 1.29	14.8 ± 1.71*	6.75 ± 0.96*	10.0 ± 1.83 [#]	7.0 ± 0.82* ^a	13.25 ± 3.30 [#]

Values denote the mean ± SD of ten rats/ group. * $p \leq 0.05$ vs. control, # $p \leq 0.05$ vs. PbAc-induced group, and ^a $p < 0.05$ vs. PbAc + MIX group using ANOVA (one-way)

or ZnO-NPs to PbAc-exposed rats resulted in a significant increase ($p < 0.05$) in seminal fructose levels paralleled with infertile rats. The control groups treated with 10-HAD and ZnO-NPs exhibited no significant alterations in seminal fructose levels compared to sham control. In contrast, the control group of rats that were administered the MIX (10-HAD and ZnO-NPs) exhibited a statistically significant reduction ($p < 0.05$) in seminal fructose levels when compared to the sham control group (Fig. 3B).

The Impact of Lead Acetate Exposure and Different Treatments on Testicular Lead Content Among the Investigated Groups

Figure 4A shows variations in testicular lead levels among the various experimental groups. The PbAc-induced group exhibited a statistically significant increase ($p < 0.05$) in testicular lead content when compared to the sham group. The administration of 10-HDA and/or ZnO-NPs to PbAc-toxified rats resulted in significant ($p < 0.05$) reductions in testicular lead levels, with a more pronounced reduction observed in the MIX treatment compared to PbAc-induced rats. Furthermore, the rats that received treatment exhibited a statistically significant increase ($p < 0.05$) in comparison to the rats in the sham group. No statistically significant differences in testicular lead levels were observed in the control-treated groups (10-HDA and/or ZnO-NPs) compared to the sham group.

The Impact of Lead Acetate Exposure and Different Treatments on Pituitary/Gonadal Hormones Among the Investigated Groups

The study revealed a significant decrease ($p < 0.05$) in serum levels of FSH, LH, and testosterone in the PbAc-testicular intoxicated group compared to the sham group (Fig. 4B and

C). Nevertheless, 10-HDA and/or ZnO-NPs treatments caused a significant elevation ($p < 0.05$) in the levels of these hormones compared with PbAc-intoxified rats. Regarding healthy rats receiving the single or combined treatments, a significant ($p < 0.05$) reduction in serum FSH level was associated with 10-HDA treatment. In contrast, ZnO-NP administration caused a significant decline ($p < 0.05$) in serum testosterone levels compared to the sham group. However, the MIX therapy did not cause any significant changes in the serum levels of FSH, LH, and testosterone compared to sham rats (Fig. 4B and C).

The Impact of Lead Acetate Exposure and Different Treatments on Testicular Antioxidant and Lipid Peroxidation Biomarkers Among the Investigated Groups

Comparative analysis revealed notable changes in the oxidative stress indices between rats treated with PbAc and the sham rats. The testicular activity of superoxide dismutase (SOD) and glutathione (GST), as well as the GSH content, exhibited a statistically significant decrease ($p < 0.05$) (Table 3). Conversely, the oxidative stress markers exhibited a significant improvement ($p < 0.05$) following the administration of 10-HDA and/or ZnO-NPs treatments. No significant alterations in the antioxidant markers were observed in the majority of control rats that received treatments. Furthermore, it was observed that rats exposed to PbAc exhibited a statistically significant increase ($p < 0.05$) in the lipid peroxidation indicator (MDA) when compared to the control group. In contrast, the administration of either the single or mixed treatments resulted in a statistically significant decrease ($p < 0.05$) in MDA levels in rats that received PbAc. Alternatively, administration of the single or mixed treatments caused a significant decline ($p < 0.05$) in MDA levels in rats

Fig. 4 The impact of lead acetate exposure and different treatments on testicular lead content (A) and serum pituitary/gonadal hormones, including follicle-stimulating hormone (FSH) and luteinizing hormone (LH) (B), and testosterone (C). Data are presented as mean \pm standard deviation ($n = 10$). *: significant ($p < 0.05$) compared to the sham group, #: significant ($p < 0.05$) compared to the PbAc-induced group, ^a: significant ($p < 0.05$) compared to the PbAc + MIX group. 10-HDA, 10-hydroxydecanoic acid (5 mg/kg/day); ZnO-NPs, zinc oxide nanoparticles (5 mg/kg/day); MIX, mixture of 10-hydroxydecanoic acid + zinc oxide nanoparticles; PbAc, lead acetate (30 mg/kg/day); PbAc + 10-HDA, lead acetate + 10-hydroxydecanoic acid; PbAc + ZnO-NPs, lead acetate + zinc oxide nanoparticles; PbAc + MIX, lead acetate + mixture of 10-hydroxydecanoic acid + zinc oxide nanoparticles

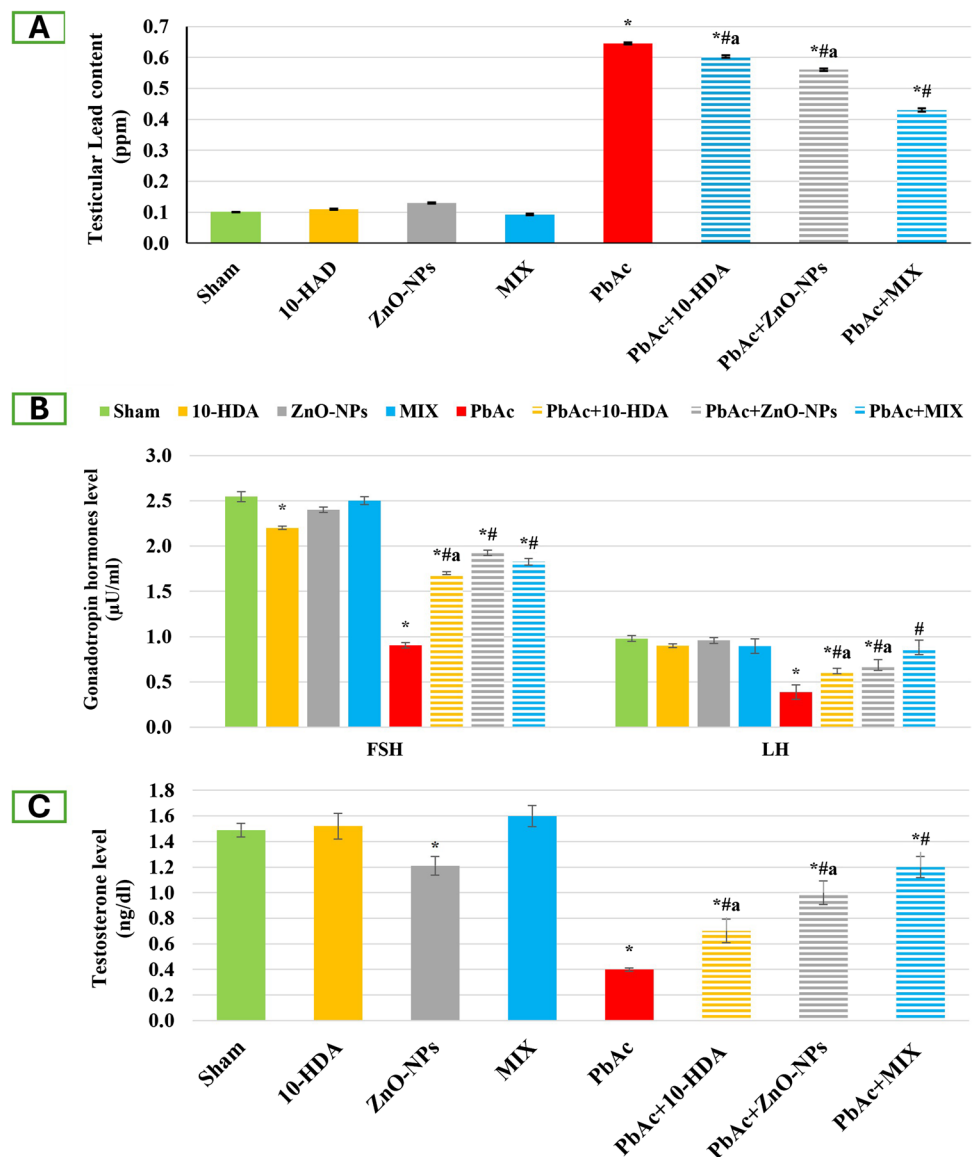


Table 3 The impact of lead acetate exposure and different treatments on testicular antioxidant and lipid peroxidation biomarkers

Parameters	Sham	10-HDA	ZnO-NPs	MIX	PbAc	PbAc + 10-HDA	PbAc + ZnO-NPs	PbAc + MIX
SOD (U/mg protein)	266.48 \pm 0.51	262.65 \pm 1.29	251.00 \pm 0.70*	287.10 \pm 0.97*	141.74 \pm 0.30*	236.83 \pm 1.31* ^a	242.80 \pm 0.21* ^a	260.20 \pm 2.20 [#]
GST (U/mg protein)	740.60 \pm 27.85	671.00 \pm 15.87*	735.60 \pm 11.93	644.10 \pm 32.63*	454.11 \pm 26.84*	629.91 \pm 24.54* [#]	570.00 \pm 28.60* ^a	624.60 \pm 21.21* [#]
GSH (mM/mg protein)	3.55 \pm 0.13	3.93 \pm 0.36	3.78 \pm 0.17	3.70 \pm 0.22	1.90 \pm 0.29*	2.85 \pm 0.13* ^a	3.63 \pm 0.78 [#]	3.43 \pm 0.42 [#]
MDA (mM/mg protein)	0.16 \pm 0.05	0.19 \pm 0.04	0.18 \pm 0.02	0.16 \pm 0.01	0.23 \pm 0.01*	0.21 \pm 0.04	0.21 \pm 0.04	0.16 \pm 0.03 [#]

Data correspond to the mean \pm SD of ten rats/ group. * $p \leq 0.05$ vs. control, # $p \leq 0.05$ vs. PbAc-induced group, and ^a $p < 0.05$ vs. PbAc + MIX group using ANOVA (one-way), $n = 10$

receiving PbAc, where the mixed treatment exhibited greater efficacy. Single or combined-treated control rats did not display any significant change in MDA level compared to the sham rats (Table 3).

Figure 5A–C shows changes in testicular protein content of Nrf2 and HO-1 associated with the various treatments. The PbAc-exposed group exhibited a significant decrease ($p < 0.05$) in Nrf2 and HO-1 protein levels compared to healthy animals. The different treatment regimens (10-HDA and/or ZnO-NPs) resulted in a significant elevation ($p < 0.05$) in Nrf2 and HO-1 protein levels compared to rats exposed to PbAc only. The combined treatment demonstrated greater efficacy in increasing the expression levels of Nrf2 and HO-1. Nonetheless, the protein content of Nrf2 and HO-1 after these treatments remained significantly lower ($p < 0.05$) compared to sham rats. While individual administrations of 10-HDA or ZnO-NPs to healthy rats resulted in statistically significant reductions ($p < 0.05$) in Nrf2 and HO-1 expression levels compared to sham rats, the combined treatment did not yield significant effects (Fig. 5A–C).

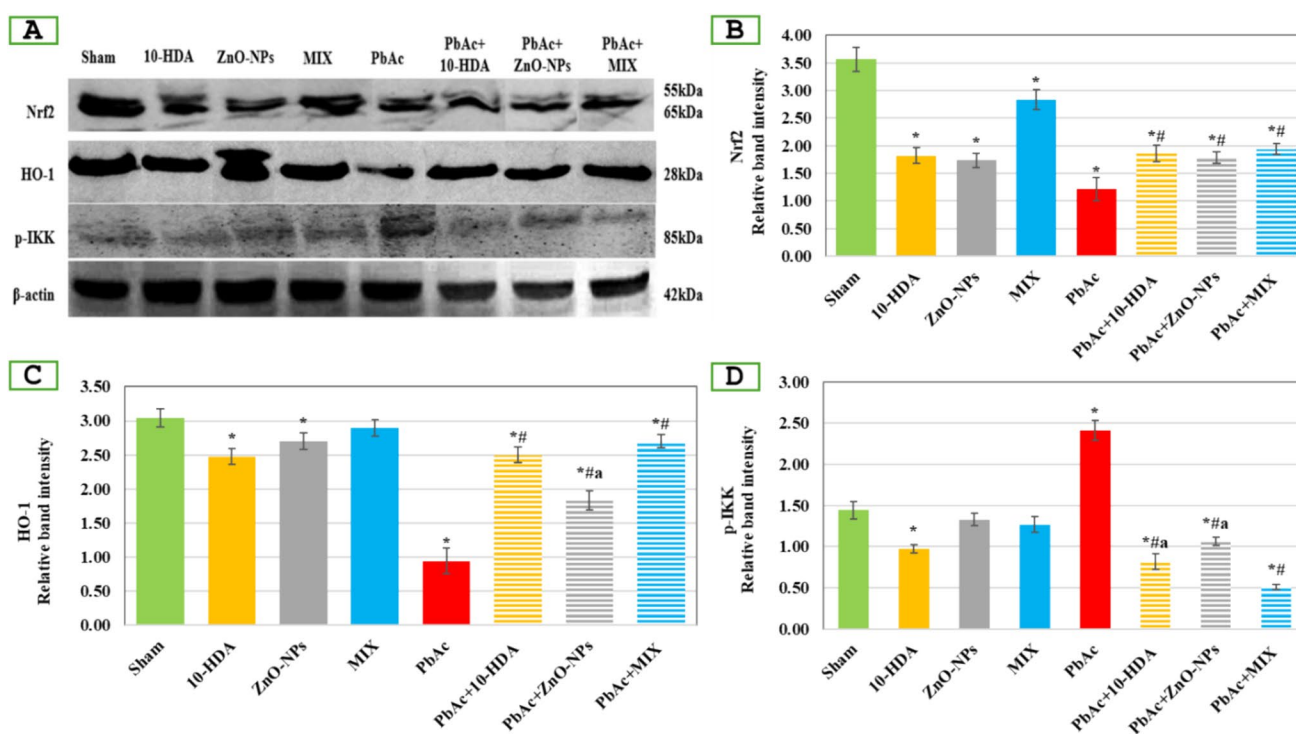


Fig. 5 Western blot analysis of testicular nuclear factor erythroid 2-related factor 2 (Nrf2), heme oxygenase-1 (HO-1), and phosphorylated inhibitor of nuclear factor κ B kinase (p-IKK) in the different experimental groups. (A) The western immunoblots. (B–D) Relative intensity of the protein bands analyzed by densitometry. β -actin was probed as an internal control for relative intensity analysis. Data is shown as mean \pm standard deviation ($n = 3$). *: significant ($p < 0.05$) compared to the sham group, #: significant ($p < 0.05$)

The Impact of Lead Acetate Exposure and Different Treatments on Testicular Inflammatory Markers Among the Investigated Groups

Figure 5D displays the levels of testicular p-IKK protein for each of the designed groups. In comparison to the sham rats, a statistically significant increase ($p < 0.05$) in the expression level of p-IKK protein was observed in rats receiving PbAc. Nevertheless, the observed increase was notably reduced ($p < 0.05$) by the various intervention protocols (10-HDA and/or ZnO-NPs). Furthermore, the administration of 10-HDA to healthy rats resulted in a statistically significant ($p < 0.05$) reduction in the expression level of p-IKK. In contrast, the other control groups did not exhibit any significant differences when compared to the sham control.

Additionally, as depicted in Fig. 6, the exposure to PbAc resulted in the initiation of testicular inflammation, as evidenced by the statistically significant ($p < 0.05$) increases in the levels of inflammatory markers, namely IL-1 β , IL-6, IL-8, TNF- α , and NO, when compared to the control group. In contrast, the administration of 10-HDA and ZnO-NPs, either individually or in combination, to rats induced with

compared to the PbAc-induced group, ^a: significant ($p < 0.05$) compared to the PbAc+MIX group. 10-HDA, 10-hydroxydecanoic acid (5 mg/kg/day); ZnO-NPs, zinc oxide nanoparticles (5 mg/kg/day); MIX, mixture of 10-HDA+ZnO-NPs; PbAc, lead acetate (30 mg/kg/day); PbAc+10-HDA, lead acetate+10-hydroxydecanoic acid; PbAc+ZnO-NPs, lead acetate+zinc oxide nanoparticles; PbAc+MIX, lead acetate+mixture of 10-HDA+ZnO-NPs

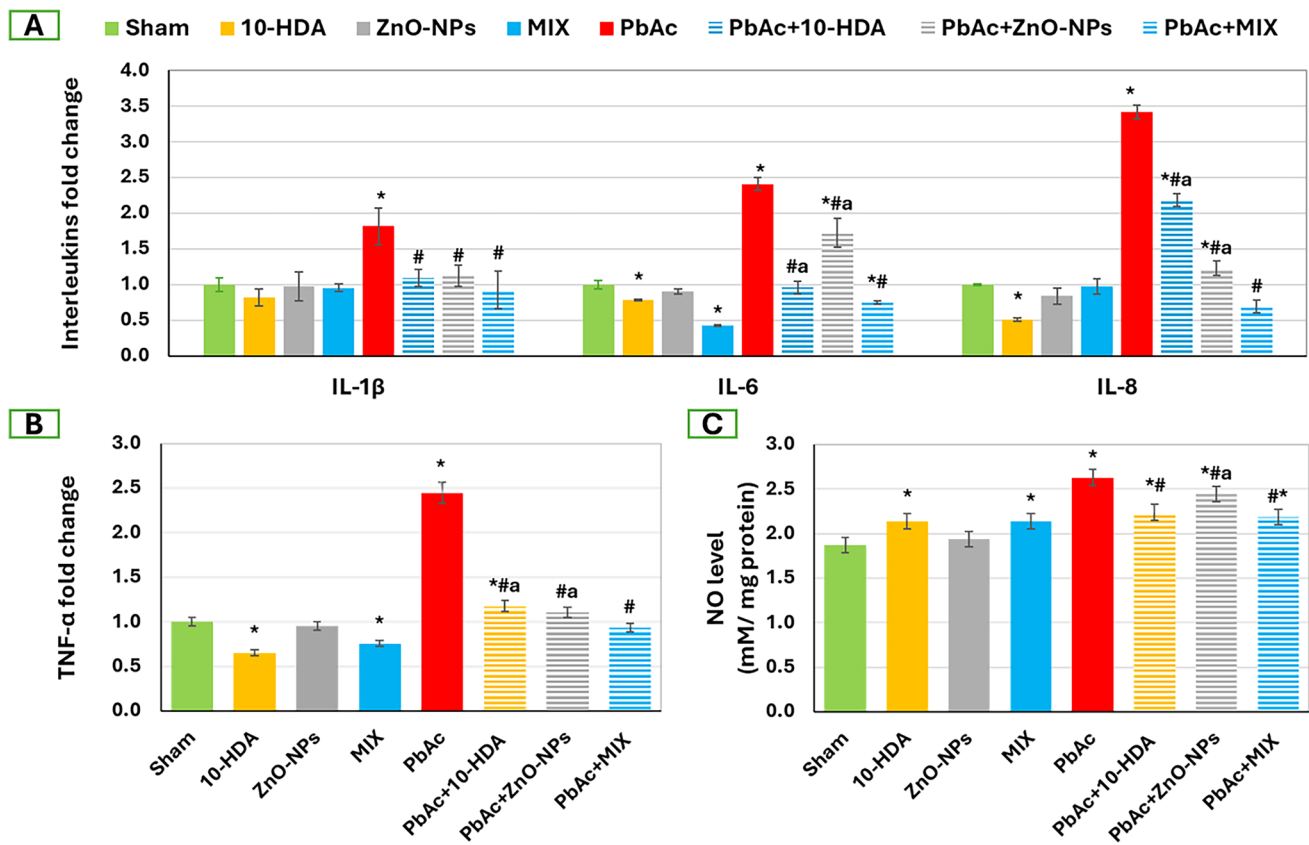


Fig. 6 The impact of lead acetate exposure and different treatments on testicular inflammatory markers. (A) Interleukins fold change (IL-1 β , IL-6, and IL-8), (B) TNF- α fold change, and (C) NO level. Data is shown as mean \pm standard deviation ($n=4$). *: significant ($p < 0.05$) compared to the sham group, #: significant ($p < 0.05$) compared to the PbAc-induced group, #: significant ($p < 0.05$) compared to the PbAc+MIX group. 10-HDA, 10-hydroxydecanoic

acid (5 mg/kg/day); ZnO-NPs, zinc oxide nanoparticles (5 mg/kg/day); MIX, mixture of 10-hydroxydecanoic acid+Zinc oxide nanoparticles; PbAc, lead acetate (30 mg/kg/day); PbAc+10-HDA, lead acetate+10-hydroxydecanoic acid; PbAc+ZnO-NPs, lead acetate+zinc oxide nanoparticles; PbAc+MIX, lead acetate+mixture of 10-hydroxydecanoic acid+zinc oxide nanoparticles

PbAc resulted in statistically significant reductions ($p < 0.05$) in these levels when compared to the PbAc-toxified rats that did not receive any treatments. Interestingly, the MIX treatment exhibited a greater efficacy in reducing the markers of inflammation. Most of the control treatments with 10-HDA and/or ZnO-NPs exhibited a significant reduction ($p < 0.05$) in the examined inflammatory markers compared to control rats receiving saline.

The Impact of Lead Acetate Exposure and Different Treatments on Testicular Apoptotic and Survival Responses Among the Investigated Groups

Rats receiving PbAc demonstrated a significant elevation ($p < 0.05$) in Bax and caspase-3 expression levels compared to the sham group. However, these levels were significantly ($p < 0.05$) reverted in PbAc-treated rats receiving 10-HDA, ZnO-NPs, or MIX compared with PbAc-infertility rats. The controls receiving the treatment protocols

showed significant differences ($p < 0.05$) compared to the healthy untreated rats. Regarding the survival marker (Bcl-2), PbAc caused a significant ($p < 0.05$) drop in its expression level compared to the sham rats. Conversely, the administration of 10-HDA and ZnO-NPs individually or in combination resulted in a statistically significant increase ($p < 0.05$) in the expression of Bcl-2 in these rats. In comparison to the sham rats, the control group treated with ZnO-NPs did not exhibit any statistically significant differences in Bcl-2 levels.

Concerning the Bax/Bcl-2 ratio, the PbAc-treated group showed a significant rise ($p < 0.05$) compared with healthy rats. Remarkably, administration of 10-HDA and/or ZnO-NPs to PbAc-intoxified rats exhibited a significant decline ($p < 0.05$) in the Bax/Bcl-2 ratio compared to PbAc-infertility rats. Only the MIX-control group exhibited a statistically significant increase ($p < 0.05$) in the Bax/Bcl-2 ratio compared to the sham group (Fig. 7).

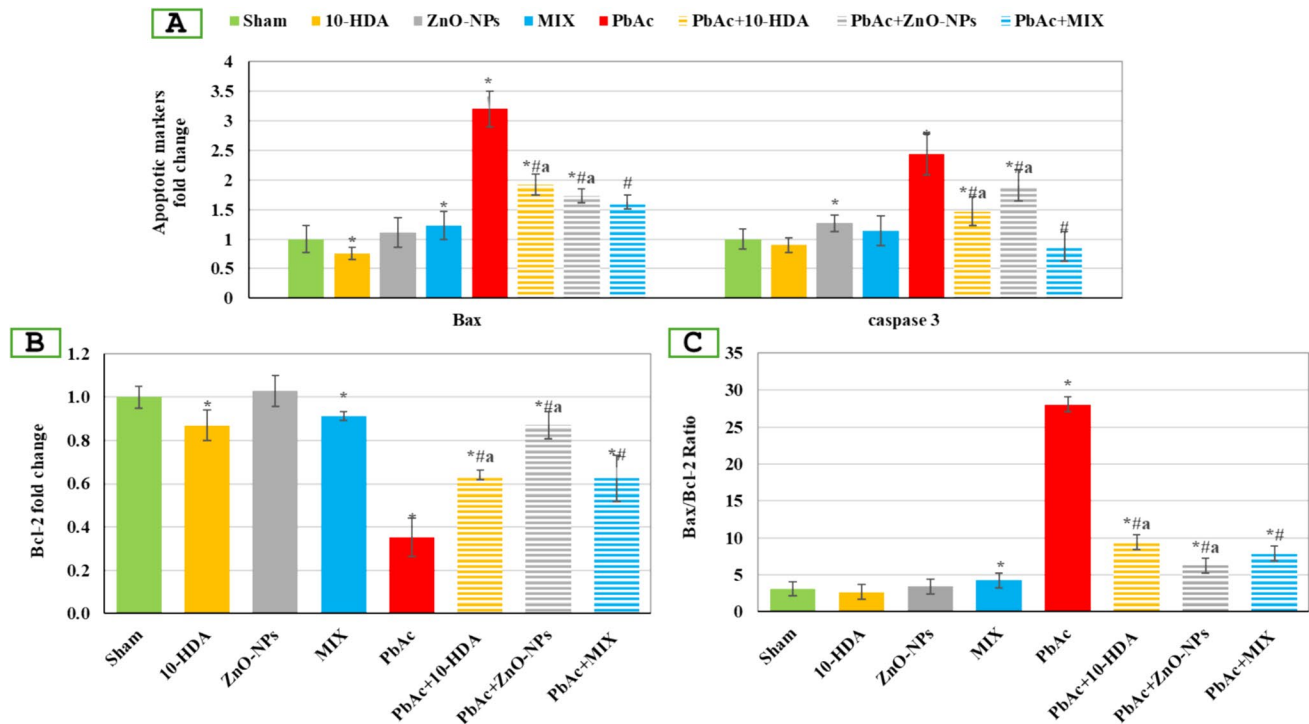


Fig. 7 The impact of lead acetate exposure and different treatments on testicular apoptotic and survival markers. (A) Bax and caspase-3 mRNA expression levels, (B) Bcl-2 mRNA expression levels, and (C) Bax/Bcl-2 ratio. Data is shown as mean \pm standard deviation ($n=4$). *: significant ($p<0.05$) compared to the sham group, #: significant ($p<0.05$) compared to the PbAc-induced group, ^a: significant ($p<0.05$) compared to the PbAc+MIX group.

Synergistic Properties of 10-HAD and ZnO-NPs Combined Treatment

The combined administration of 10-HDA and ZnO-NPs demonstrated a synergistic effect ($CI < 1$) against lead acetate-induced oxidative stress, inflammation, and apoptosis actions in rats' testicular tissues (Table 4).

The Impact of Lead Acetate Exposure and Different Treatments on Testicular Histoarchitecture

Figure 8 demonstrates the testicular tissues of sham, 10-HDA, ZnO-NPs, and MIX groups. The examined samples displayed normal histological and architectural features of interstitial tissues, seminiferous tubules, Sertoli cells, Leydig cells, and spermatogenic cells. Conversely, spermatogenic cells of testicular samples from rats administering PbAc revealed anomalous arrangement, vacuolization, and degeneration. Additionally, seminiferous tubules exhibited a necrotic epithelial cell lining and a detached basement membrane. When examining the central regions of the tubular laminae, tissue samples obtained from rats induced with PbAc exhibited the presence of cellular debris, necrosis of

10-HDA, 10-hydroxydecanoic acid (5 mg/kg/day); ZnO-NPs, zinc oxide nanoparticles (5 mg/kg/day); MIX, mixture of 10-hydroxydecanoic acid+zinc oxide nanoparticles; PbAc, lead acetate (30 mg/kg/day); PbAc+10-HDA, lead acetate+10-hydroxydecanoic acid; PbAc+ZnO-NPs, lead acetate+zinc oxide nanoparticles; PbAc+MIX, lead acetate+mixture of 10-hydroxydecanoic acid+zinc oxide nanoparticles

spermatocytes, and eosinophilic proteinaceous materials. Furthermore, there is a marked decline in Sertoli cell count and expanded intertubular tissues with scarce Leydig cells spreading, along with intertubular blood vessel congestion and interstitial edema. Conversely, the earlier deteriorations and evident amendments in the testicular histological and architectural structures were ameliorated by the treatment of the PbAc-induced testicular toxicity with either or both 10-HDA and ZnO-NPs. Nevertheless, their efficacy was comparable to that of the sham limitations. The group treated with PbAc+MIX exhibited the most significant ameliorating effect.

Discussion

Lead is a heavy metal that is considered non-essential for living organisms. It possesses the ability to induce a wide range of physiological and biochemical alterations, leading to renal failure, neurological dysfunctions, impaired fertility, and eventually death [67]. Lead has the potential to cause male infertility through various mechanisms, including its interference with the production of antioxidant enzymes.

Table 4 Combination index (CI) of 10-HDA and ZnO-NPs mixture on the measured parameters

Parameters	CI	Effect	
Seminal parameters and hormone levels			
Sperm count ($10^6/ml$)	0.550 ± 0.033	Synergistic	
Morphology index (%)	0.505 ± 0.022	Synergistic	
Motility type (%)	Rapid	0.526 ± 0.013	Synergistic
	Non-progressive	0.460 ± 0.015	Synergistic
Motility (%)	1st h	0.575 ± 0.028	Synergistic
	2nd h	0.616 ± 0.037	Synergistic
	3rd h	0.779 ± 0.034	Synergistic
Seminal fructose level (mg/g tissue)	0.466 ± 0.022	Synergistic	
FSH ($\mu U/ml$)	0.507 ± 0.058	Synergistic	
LH ($\mu U/ml$)	0.671 ± 0.054	Synergistic	
Testosterone (ng/dl)	0.700 ± 0.098	Synergistic	
Testicular lead content (ppm)	0.369 ± 0.041	Synergistic	
Oxidative stress markers			
SOD (U/mg protein)	0.543 ± 0.011	Synergistic	
GST (U/min/mg protein)	0.521 ± 0.030	Synergistic	
GSH (mM/g tissue)	0.534 ± 0.083	Synergistic	
NO (mM/mg protein)	0.496 ± 0.205	Synergistic	
MDA (mM/mg protein)	0.373 ± 0.047	Synergistic	
Nrf2 (protein expression level)	0.532 ± 0.015	Synergistic	
HO-1 (protein expression level)	0.624 ± 0.027	Synergistic	
Inflammatory markers			
p-IKK (protein expression level)	0.270 ± 0.071	Synergistic	
IL-1 β (mRNA fold change)	0.488 ± 0.057	Synergistic	
IL-6 (mRNA fold change)	0.318 ± 0.039	Synergistic	
IL-8 (mRNA fold change)	0.239 ± 0.081	Synergistic	
TNF- α (mRNA fold change)	0.474 ± 0.042	Synergistic	
Apoptotic markers			
Caspase-3 (mRNA fold change)	0.304 ± 0.059	Synergistic	
Bcl-2 (mRNA fold change)	0.498 ± 0.058	Synergistic	
Bax (mRNA fold change)	0.513 ± 0.025	Synergistic	

CI value of < 1 indicates synergistic effect; > 1 indicates antagonistic effect; $= 1$ indicates additive effect. Values are means \pm SD

It increases free radicals production, impairs signaling pathways, provokes apoptosis, increases inflammation, causes cellular dysfunction, and impedes endocrine function through the hypothalamus-pituitary-testes axis [68, 69]. Additionally, lead is well known for its low elimination rate, thereby promoting its accumulation within the human body [70]. Lead accumulation in reproductive tissues can compromise the integrity of the blood-testis barrier, which is predominantly reinforced by the tight junctions present in Sertoli cells. Consequently, the compromised blood-testis barrier facilitates lead entry into the seminiferous tubules, amplifying lead toxicity [71]. In the current study, a substantial elevation in the testicular lead content was observed, accompanied by a depleted sperm count, morphology index, and motility, in rats exposed to PbAc. Furthermore, PbAc

exposure resulted in histopathological alterations in testicular tissues represented by epithelium vacuolization, diminished diameter of seminiferous tubules, elevated apoptosis of germ cells, impaired spermatogenesis, and substantial maturation arrest [72, 73]. These findings provide further support for previous studies indicating that the accumulation of lead in testicular tissues and the disruption of lead homeostasis in male reproductive organs can have detrimental effects on the integrity of the blood-testis barrier, sperm production and morphology, sperm count, sperm motility, and the rate of DNA damage in sperm cells [74–78].

The current study aimed to determine the curative effect of 10-HDA and its combination with ZnO-NPs on male infertility, testicular antioxidants, reproductive hormones, pro-inflammatory and pro-apoptotic gene expression, and

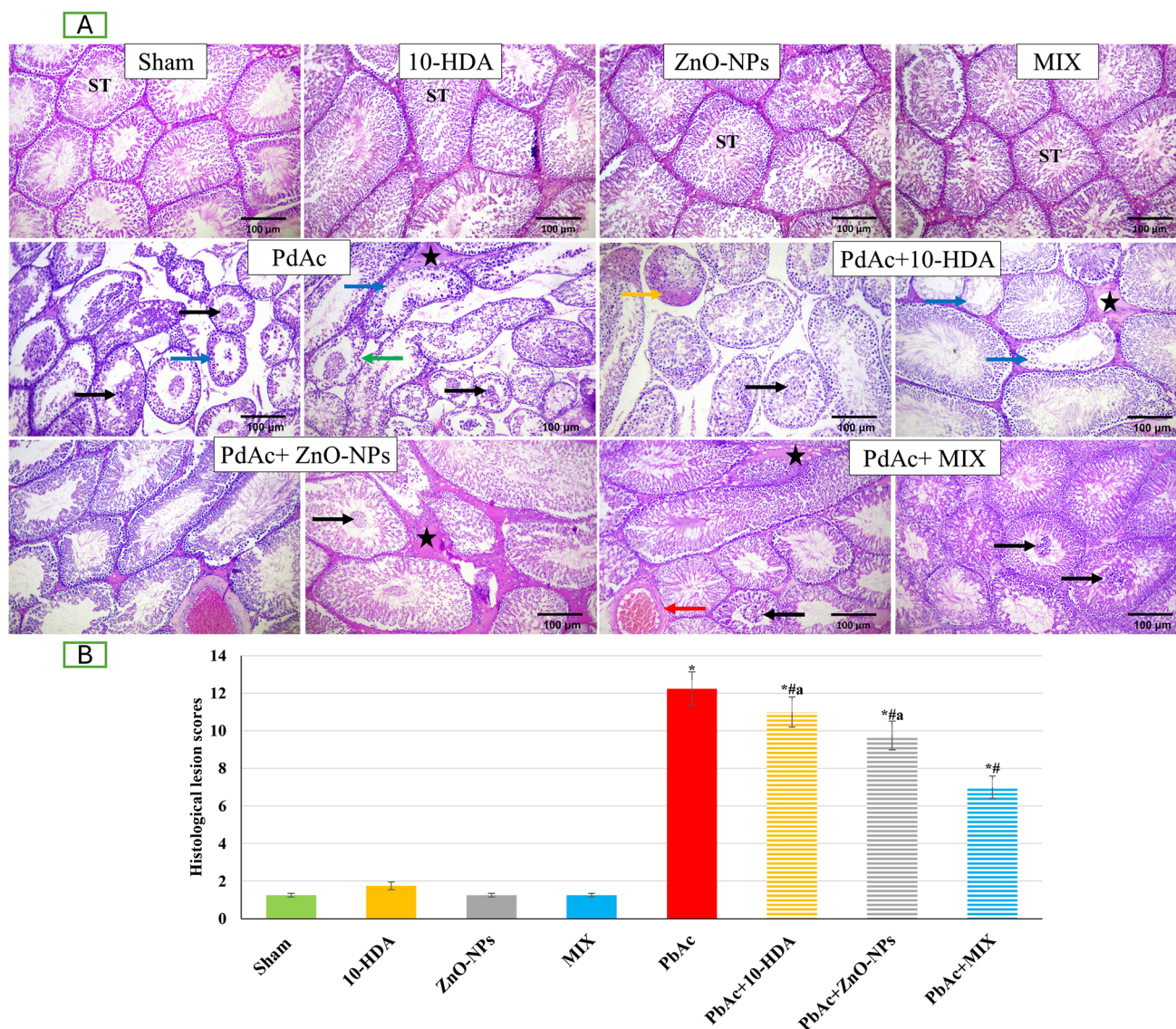


Fig. 8 Representative photomicrographs demonstrating the histopathological changes in the rat testicular tissues of different groups. (A) H&E stained sections ($\times 100$). Normal seminiferous tubules (ST), a typical seminiferous tubules with deformed spermatogenesis and buckled tubular membrane (green arrow), sloughed deteriorated germinal epithelial cells (black arrow), diminution of the germinal epithelium of tubules (blue arrow) with necrosis and hyalinization of the luminal contents (orange arrow), congestion of interstitial vessel (red arrow) and interstitial edema (star) were detected. (B) Histological lesion score assessment across various groups. Data is shown as mean \pm standard deviation ($n=10$). p -values were

assessed by comparing them with those of the sham group. *: significant ($p < 0.05$) compared to the sham group, #: significant ($p < 0.05$) compared to the PbAc-induced group, ^a: significant ($p < 0.05$) compared to the PbAc+MIX group. 10-HDA, 10-hydroxydecanoic acid (5 mg/kg/day); ZnO-NPs, zinc oxide nanoparticles (5 mg/kg/day); MIX, mixture of 10-hydroxydecanoic acid+zinc oxide nanoparticles; PbAc, lead acetate (30 mg/kg/day); PbAc+10-HDA, lead acetate+10-hydroxydecanoic acid; PbAc+ZnO-NPs, lead acetate+zinc oxide nanoparticles; PbAc+MIX, lead acetate+mixture of 10-hydroxydecanoic acid+zinc oxide nanoparticles

histopathology. This study hypothesized that the 10-HDA and ZnO-NPs could have beneficial effects on the male rat reproductive system compared to their monotherapy. ZnO-NPs possess distinctive physical and chemical characteristics that facilitate their interaction with cellular macromolecules and elicit a range of medicinal effects through expressing

antioxidants, antibacterial, anticancer, and anti-inflammatory potentials [79–82]. Goma [49] demonstrated that ZnO-NPs at a low dose of 5 mg/kg can have a positive impact on male fertility. However, high doses (50, 150, 300, and 350 mg/kg) may function as testicular toxicants in mice [49, 83]. 10-HDA has a stable structure in RJ that is free of

double bonds [28]. Several studies reviewed the favorable functions of RJ on male fertility [23, 84, 85]. Oral administration of RJ (100 mg/kg) in diet before sexual maturity improved semen quality and sexual behavior of male rabbits [84]. Furthermore, the antioxidant properties of RJ facilitate the mitigation of cellular toxicity in testicular tissue and protect the integrity of the testicular structure against the detrimental impacts of doxorubicin [86] and diabetic oxidative stress [85], hence preserving male fertility. The present study demonstrates that the administration of 10-HDA and/or ZnO-NPs resulted in a reduction in testicular lead content, indicating the chelating activity of our treatment and subsequent lead clearance from the testes. Remarkably, the combined treatment exhibited a synergistic activity by effectively lowering lead content in testicular tissues. Additionally, the treatments significantly improved sperm count, morphology index, and motility and were able to improve the architecture of testicular tissues. In agreement with our findings, Afifi [87] illustrated that ZnO-NPs (10 mg/kg), either alone or in combination with insulin, can increase sperm count and motility and shield testicular tissue from oxidative stress in diabetic rats. Moreover, the co-administration of green ZnO-NPs showed adequate protective effects against the induced testicular damage [50].

Sperm functionality is adversely affected when ROS levels surpass the physiological threshold, which is necessary for normal sperm functioning [3, 88]. The toxicity of lead is associated with an increase in oxidative stress, resulting in harm to DNA, proteins, and lipids. These detrimental effects can accelerate the deterioration of both the functionality and structure of the testes, ultimately leading to cell death and involvement in various diseases [78]. Lead can trigger oxidative stress by two routes: the amplified production of ROS and the impact of lead on the antioxidant defense system [89]. The excessive production of ROS is amalgamated with various male fertility matters, for example, varicocele and leukocytopenia [3, 88, 90]. In the present study, rats receiving PbAc demonstrated a decline in the activity of SOD and GST, as well as the content of the antioxidant GSH, indicating a compromised antioxidant defensive system. These outcomes align with the preceding findings [91, 92]. Conversely, 10-HDA and ZnO-NPs therapies could alleviate testicular tissue oxidative stress by increasing SOD and GST activities and GSH content along with reduced MDA levels. The antioxidant properties of these treatments may be responsible for these recoveries. In two microglial models, 10-HDA was reported to suppress the production of ROS, which was induced by lipopolysaccharide (LPS), in a dose-dependent manner [22]. Additionally, RJ (100 mg/kg/day, for 35 days) was reported to effectively protect the

testis against nicotine-induced testicular damage through upregulation of the antioxidant activity, prevention of mitochondria-dependent apoptosis, and the improvement of proliferating activity [93]. Zinc is a cofactor for approximately 300 enzymes that play a variety of significant activities, primarily those that are engaged in the antioxidant defense process. Zinc serves as a sulfhydryl group protector, preventing it from adhering to catalytic sites, and is essential for the activation of antioxidant enzymes and proteins, such as catalase, SOD, and glutathione [94, 95]. In ZnO-NPs treated diabetic rats, Afifi [87] demonstrated increased SOD, GST, glutathione peroxidase, glutathione reductase, and catalase activity and mRNA expression. Moreover, testicular tissue MDA decreased, while GSH increased. Additionally, Majd [50] illustrated that the co-administration of green ZnO-NPs (5 mg/kg) restored the suppressive effects of cisplatin-induced reproduction toxicity on the activities of the antioxidant enzymes (SOD, glutathione peroxidase, and catalase). Therefore, low doses of 10-HDA and ZnO-NPs improved the antioxidant status of the testicular tissue, reduced free radical levels, and shielded the integrity of the cell membrane from the damaging effects of oxidative stress.

Additionally, Nrf2 and HO-1 constitute a vital pathway that protects against various environmental and internal stressors [96]. The protein Nrf2, which plays a crucial role in regulating antioxidant proteins, is generally rendered inactive through its interaction with the cytoplasmic complex. However, upon cellular damage, Nrf2 gets translocated into the nucleus to stimulate the production of a variety of phase II detoxification and antioxidant enzymes, such as glutathione reductase, NAD(P)H quinone dehydrogenase-1 (NQO-1), and HO-1. These enzymes mitigate oxidative stress in cells and tissues [97, 98]. This study demonstrated reduced protein levels of Nrf2 and HO-1 in the testes of the PbAc-intoxicated group. These results align with previous findings [99, 100]. Alternatively, 10-HDA and ZnO-NPs treatments restored Nrf2 and HO-1 protein levels, reflecting these treatments' ability to reestablish the antioxidant defense system through reactivating the Nrf2/HO-1 signaling pathway. Consistent with these findings, Almeer [101] deduced that RJ administration minimized the Cd-induced testicular toxicity and oxidative stress through the upregulation of Nrf2 and HO-1. The study of Awadalla [98] indicated that intraperitoneal injection of ZnO-NPs (5 mg/kg, 3 times/week, for 8 weeks) up-regulated antioxidant genes (Nrf2 and HO-1) in the induced-chronic kidney disease rats.

Mitochondrial dysfunction is associated with disrupted steroidogenesis and spermatogenesis. Lead could induce mitochondrial impairment by triggering oxidative stress, mitochondrial membrane depolarization, and

permeabilization while inhibiting enzymes involved in energy metabolism [102]. Moreover, the significant amount of polyunsaturated fatty acids (PUFA) and the abundance of mitochondria in spermatozoa render them more susceptible to oxidative stress [103]. ROS can impair sperm viability, morphology, motility, and capacity by inducing oxidative DNA strand breaks, mitochondrial dysfunction, and PUFA peroxidation. These detrimental effects can cause metabolic dysfunction of Sertoli cells, thus impairing spermatogenesis [104, 105]. The current investigation revealed that exposure to PbAc resulted in a notable decrease in sperm count, morphology index, and motility characteristics. Furthermore, PbAc induced an increase in testicular MDA, which is the main reaction product of lipid peroxidation. These changes are supported by previous investigations [16, 106–108]. Treating rats with 10-HDA and/or ZnO-NPs produced a profound enhancement in sperm count, morphology index, motility, and decreased MDA levels. RJ's improved activity on sexual behavior and semen quality was previously reported as contributing to its antioxidant properties [84–86, 109]. ZnO-NPs represent a valuable and safe additive material that is effective at reducing peroxidative damage during sperm cryopreservation and improving semen quality by acting as antioxidants [82, 110, 111]. Interestingly, Majd [50] reported that the co-administration of green ZnO-NPs to cisplatin-induced reproduction toxicity significantly elevated sperm count and progressive motility, while this increasing effect was not observed in ZnO bulk and chemical ZnO-NPs. This finding is compatible with the synergetic effect of the current combination of ZnO-NPs with 10-HAD. The preventive and ameliorative effects of 10-HAD and ZnO-NPs on sperm parameters can be attributed to their antioxidant and free radical scavenging ability.

Seminal fructose is the key energy source for spermatozoa. It serves as a marker of seminal vesicle function [112]. Lead can lower seminal fructose, which can be related to the ability of lead to replace metal cofactors of different enzymes involved in the biosynthesis of fructose [105, 113]. In contrast, the application of 10-HDA and/or ZnO-NPs agents effectively reversed the decrease in seminal fructose levels resulting from exposure to PbAc. This finding could potentially be elucidated by the antioxidant capacity of our therapeutic interventions, as prior research has established a correlation between reduced seminal fructose levels and the occurrence of oxidative stress [105, 112, 114]. Furthermore, the administered remedies possess chelating properties that effectively reduce the levels of lead in the testes, thereby facilitating the restoration of enzymatic activity involved in fructose synthesis.

Another mechanism that contributes to male infertility is testicular inflammation [115]. Oxidative stress is immensely

implicated in the development of inflammation. This result can be explained by the ability of reactive oxygen/nitrogen species to activate intracellular signaling pathways that encourage the activation of pro-inflammatory responses [116]. Furthermore, inflammatory mediators can activate and recruit immune cells to the inflammatory site. These cells induce an excessive release of reactive species, intensifying oxidative stress [117]. Besides, NO produced by iNOS during oxidative stress can aggravate inflammation by amplifying NF- κ B signaling [118–120]. NF- κ B signaling pathway controls the expression of pro-inflammatory cytokines and chemokines. In the cytoplasm, I κ B sequesters NF- κ B, thereby inhibiting its activity. TNF- α activates NF- κ B signaling through phosphorylating IKK, which sequentially phosphorylates I κ B, causing its degradation and releasing NF- κ B to initiate target gene transcription [121]. In this investigation, PbAc exposure caused an increase in testicular NO content, escorted by a rise in the expression of p-IKK, IL-1 β , IL-6, IL-8, and TNF- α . This finding is consistent with previous studies reporting the stimulation of the NF- κ B pathway accompanied by an increase in inflammatory cytokines in testicular tissue following lead administration [102, 122–126].

In contrast, previous studies reported the anti-inflammatory activity of 10-HDA by hindering the NF- κ B pathway and the expression of pro-inflammatory cytokines [22, 118, 127]. The study of You [22] revealed that the increased iNOS, IL-1 β , IL-6, and TNF- α levels were suppressed by the 10-HDA pretreatment associated with a concentration-dependent decrease in NO levels compared to LPS-induced inflammation. Furthermore, the anti-inflammatory properties of ZnO-NPs were demonstrated through the reduction of NF- κ B signaling and the subsequent decrease in pro-inflammatory cytokines. Moreover, the utilization of ZnO-NPs has been shown to inhibit the expression of iNOS, thereby reducing inflammation [128, 129]. Goma [49] and Awadalla [98] reported down-regulated inflammatory genes (IL-6 and TNF- α) in ZnO-NP-treated rats. In consistence, the present treatments involving 10-HDA and/or ZnO-NPs reduced the levels of p-IKK and the pro-inflammatory mediators. Therefore, we postulate that the inhibition of the NF- κ B pathway may be involved in the mechanism by which 10-HDA and ZnO-NPs exert their anti-inflammatory effects.

The hypothalamic-pituitary–testicular axis can be negatively impacted by lead-induced oxidative stress and inflammation, which can lead to the inhibition of testosterone production and spermatogenesis through the induction of gonadotropin-inhibitory hormone expression [104, 130]. Moreover, lead can hamper the hormonal feedback pathways in the reproductive hormonal axis by dysregulating LH and FSH production. Oxidative stress and inflammation

are correlated with elevated prolactin, exerting a negative feedback loop on LH, FSH, and testosterone production, reducing spermatogenesis [131]. Additionally, lead can directly hinder testicular steroidogenesis by impeding Leydig cell differentiation, which is responsible for the production of testosterone [132]. Consistent with previous findings, PbAc-exposed rats displayed a significant decline in the blood sex hormone levels (testosterone, LH, and FSH) [108, 133, 134]. 10-HDA and/or ZnO-NPs administration revealed a notable rise in testosterone, FSH, and LH levels compared to PbAc-exposed rats. The observed decline in activity may be attributed to oxidative stress induced by a reduction in the efficacy of antioxidant species. Hence, the observed enhancement could potentially be attributed to the potent antioxidant characteristics exhibited by these compounds. Furthermore, the administration of RJ not only mitigates reproductive tract impairment resulting from various detrimental stressors but also enhances the production of male hormones, thereby leading to improvements in sperm count, motility, and morphology [23, 85]. Moreover, there are numerous important biological hormone interactions with zinc. Zinc improved the passivity of organ reactivity and receptor locations and had a role in hormone synthesis, storage, and discharge. Furthermore, it is worth noting that zinc oxide (ZnO) plays a vital role in the synthesis of various sex hormones, including testosterone. The utilization of ZnO as a zinc source may contribute to raising testosterone concentrations [49, 135]. Additionally, Mozaffari [136] stated that ZnO-NPs caused a substantial rise in FSH and testosterone levels. The two intracellular mechanisms by which ZnO-NPs increase LH and FSH are described. One factor contributing to the observed phenomenon is the increased levels of zinc in the pituitary gland. These elevated zinc levels disrupt the release of dopamine from the pituitary gland, consequently reducing the indirect inhibitory effect of dopamine on the gonadotropin-releasing hormone (GnRH). The second mechanism involved the direct inhibition of the gamma-aminobutyric acid (GABA) nerve system by ZnO-NPs [136].

Furthermore, oxidative stress can trigger apoptosis by disrupting the permeability of the mitochondrial membrane. This leads to the liberation of cytochrome c into the cytosol, activating the caspase cascade and promoting apoptotic cell death [137, 138]. One of the anti-apoptotic proto-oncogenes is Bcl-2. Bcl-2 maintains the integrity of the mitochondrial membrane during intrinsic apoptosis. Therefore, the reduction in Bcl-2 expression/stability leads to releasing of cytochrome c through the mitochondrial membrane, resulting in caspase-dependent apoptosis [93]. In line with our findings, PbAc exposure was found to induce apoptosis by enhancing the transcription of the pro-apoptotic Bax and caspase-3 while decreasing the transcription

of the anti-apoptotic Bcl-2 in the testicles [125, 139, 140]. The present investigation demonstrated that low doses of 10-HDA and/or ZnO-NPs exhibited anti-apoptotic properties, as indicated by the restoration of the Bax/Bcl-2 ratio and a reduction in the expression level of caspase-3. Similarly, these studies revealed that RJ can modulate oxidative stress, inflammation, and apoptosis and prevent testicular [93], hepato-, and renal [141, 142] toxicity in rats. ZnO-NP anti-apoptotic action was also illustrated [49]. These positive effects can be attributed to the antioxidant and anti-inflammatory properties of our treatments, which enhance their effectiveness through a synergistic combination [143]. Conversely, a single intraperitoneal injection of high-dose ZnO-NPs (700 mg/kg) [49] and daily oral administration of ZnO-NPs (50 mg/kg) for 50 consecutive days [83] have apoptotic effects on spermatogenic cells and resulted in reduced sperm motility and elevated sperm abnormalities. Therefore, it is necessary to ensure sufficient intake of ZnO-NPs in order to maintain the optimal functionality of the testicles.

Conclusion

PbAc exposure induces an increase in oxidative stress, resulting in inflammation, testicular damage, and cell death through NF- κ B activation and Nrf2/HO-1 inhibition in testicular tissues (Fig. 9). The current study was the first to investigate the impact of 10-HDA and its combination with ZnO-NPs on male reproductive function, hormone levels, antioxidant levels, anti-inflammatory gene expression, and testicular histopathology. The results revealed that 10-HDA and ZnO-NPs at 5 mg/kg improved the semen characteristics, reproductive hormones, and lead clearance, increased testicular antioxidant activity, and the mRNA expression of the different anti-inflammatory and anti-apoptotic genes. In conclusion, the co-administration of ZnO-NPs with 10-HDA therapy demonstrated the most beneficial effect on male reproductive function compared to the use of these remedies independently. Individuals who are regularly exposed to lead will greatly benefit from this study.

Limitations: Further studies on the mechanisms of lead detoxification by 10-HDA and ZnO-NPs are necessary in order to elucidate the precise mechanism underlying the testicular ameliorative efficacy of these treatments. Moreover, an *in silico* molecular modeling study is needed to gain a comprehensive understanding of the interaction between the used remedies and various proteins. This study aims to assess the pharmacokinetics, pharmacodynamics, and tissue distribution of 10-HDA and ZnO-NPs, taking into consideration their potential future applications. However, animals were exposed to the target chemicals for a brief period in this investigation.

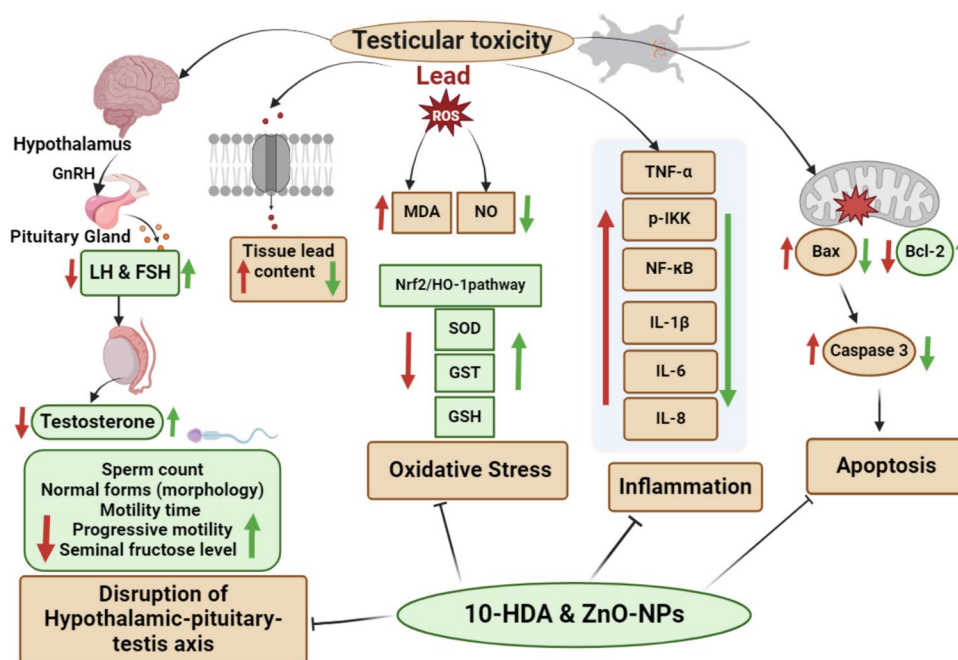


Fig. 9 Testicular toxicity as a result of chronic PbAc exposure. PbAc exposure triggers ROS production that disrupts the hypothalamic-pituitary-testis (HPT) axis, resulting in decreased levels of LH, FSH, and testosterone. In addition, it diminishes semen quality by altering sperm morphology and reducing sperm count, motility, progressive motility, and seminal fructose levels. Furthermore, PbAc exposure enhances lead accumulation in testicular tissue and promotes oxidative stress by increasing NO production and MDA levels and inhibiting the Nrf2/HO-1 pathway, leading to a reduction in antioxidant

enzymes (SOD, GST, GSH). PbAc exposure also triggers inflammatory signaling by activating TNF- α , p-IKK, NF- κ B, and ILs and initiates apoptotic action through the disruption of the caspase-3/Bax/Bcl-2 signaling pathway. The combined therapy of 10-HDA and ZnO-NPs effectively counteract these harmful effects. It restores the HPT axis function, reduces oxidative stress, inhibits inflammation, and prevents apoptosis, thereby protecting testicular function and enhancing fertility

It is possible that the prolonged use of these substances could be hazardous. Therefore, it is necessary to investigate the potential toxicity of these chemicals due to long-term use. Further research in this area may strengthen the case for a combination medicine with greater efficacy and fewer adverse effects.

Author Contribution All authors contributed to the study conception and design. A.M.M.: conceptualization; investigation; methodology; supervision; validation; visualization; data curation; writing original draft, reviewing and editing. G.A.E.: conceptualization; data curation; formal analysis; investigation; methodology; resources; validation; visualization; writing original draft and editing. S.S.E.: methodology, validation, visualization, data curation, writing the original draft and editing. D.A.G.: conceptualization; investigation; methodology; resources; supervision; reviewing and editing. S.R.S.: conceptualization; data curation; formal analysis; investigation; methodology; resources; supervision; validation; visualization; reviewing and editing. The authors declare that all data were generated in-house and that no paper mill was used. All authors read and approved the manuscript.

Funding Open access funding provided by The Science, Technology & Innovation Funding Authority (STDF) in cooperation with The Egyptian Knowledge Bank (EKB).

Data Availability The authors declare that the data supporting the findings of this study are available within the manuscript.

Declarations

Ethics Approval This study was performed in accordance with the principles outlined in the Declaration of Alexandria University Guidelines for Care and Use of Laboratory Animals. The study was approved by the Ethics Committee of Alexandria University's institutional animal care and use committee (AlexU-IACUC protocol no. AU: 04 22 10 22 1 01).

Competing Interests The authors have no relevant financial or non-financial interests to disclose.

Open Access This article is licensed under a Creative Commons Attribution 4.0 International License, which permits use, sharing, adaptation, distribution and reproduction in any medium or format, as long as you give appropriate credit to the original author(s) and the source, provide a link to the Creative Commons licence, and indicate if changes were made. The images or other third party material in this article are included in the article's Creative Commons licence, unless indicated otherwise in a credit line to the material. If material is not included in the article's Creative Commons licence and your intended use is not permitted by statutory regulation or exceeds the permitted use, you will

need to obtain permission directly from the copyright holder. To view a copy of this licence, visit <http://creativecommons.org/licenses/by/4.0/>.

References

- Aitken RJ (2024) What is driving the global decline of human fertility? Need for a multidisciplinary approach to the underlying mechanisms. *Front Reprod Health* 6:1364352
- Saleh SR, Manaa A, Sheta E, Ghareeb DA, Abd-Elmonem NM (2022) The synergetic effect of Egyptian *Portulaca oleracea* L. (Purslane) and *Cichorium intybus* L. (Chicory) extracts against glucocorticoid-induced testicular toxicity in rats through attenuation of oxidative reactions and autophagy. *Antioxidants* (Basel) 11(7)
- Pavuluri H, Bakhtary Z, Panner Selvam MK, Hellstrom WJG (2024) Oxidative stress-associated male infertility: current diagnostic and therapeutic approaches. *Medicina* 60(6):1008
- Pereira R, Sousa M (2023) Morphological and molecular bases of male infertility: a closer look at sperm flagellum. *Genes* 14(2):383
- Filipoiu DC, Bungau SG, Endres L, Negru PA, Bungau AF, Pasca B, Behl T (2022) Characterization of the toxicological impact of heavy metals on human health in conjunction with modern analytical methods. *Toxics* 10(12):716
- Ungureanu, EL and Mustatea G (2022) Toxicity of heavy metals. In: *Environmental impact and remediation of heavy metals*. IntechOpen.
- Ngu YJ, Skalny AV, Tinkov AA, Tsai CS, Chang CC, Chuang YK, Nikolenko VN, Zotkin DA, Chiu CF, Chang JS (2022) Association between essential and non-essential metals, body composition, and metabolic syndrome in adults. *Biol Trace Elem Res* 200(12):4903–4915. <https://doi.org/10.1007/s12011-021-03077-3>
- Collin MS, Venkatraman SK, Vijayakumar N, Kanimozhi V, Arbaaz SM, Stacey RGS, Anusha J, Choudhary R, Lvov V, Tovar GI, Senatov F, Koppala S, Swamiappan S (2022) Bioaccumulation of lead (Pb) and its effects on human: a review. *J Hazardous Mater Adv* 7: 100094
- Martinez-Finley EJ, Chakraborty S, Fretham S, Aschner M (2012) Admit one: how essential and nonessential metals gain entrance into the cell. *Metallomics: Integrated Biometal Sci* 4(7):593
- Slobodian MR, Petahtegoose JD, Wallis AL, Levesque DC, Merritt TJ (2021) The effects of essential and non-essential metal toxicity in the *Drosophila melanogaster* insect model: a review. *Toxics* 9(10):269
- Abd Elnabi MK, Elkaliny NE, Elyazied MM, Azab SH, Elkhalfifa SA, Elmasry S ... Abd Elaty AE (2023) Toxicity of heavy metals and recent advances in their removal: a review. *Toxics* 11(7): 580
- Raj K, Das AP (2023) Lead pollution: impact on environment and human health and approach for a sustainable solution. *Environ Chem Ecotoxicol* 5:79–85
- Ahmad, K, Shah HUR, Khan M, Iqbal A, Potrich E, Amaral L, Rasheed S, Nawaz H, Ayub A, Naseem K, Yaqoob M, Ashfaq M (2022) Lead In drinking water: adsorption method and role of zeolitic imidazole frameworks for its remediation: a review. *J Cleaner Prod* 368: 133010
- Offor SJ, Mbagwu HO, Orisakwe OE (2019) Improvement of lead acetate-induced testicular injury and sperm quality deterioration by *Solanum anomalum* thonn. ex. schumach fruit extracts in albino rats. *J Fam Reprod Health* 13(2):98
- Leal MFC, Catarino RI, Pimenta AM, Souto MRS (2023) The influence of the biometals Cu, Fe, and Zn and the toxic metals Cd and Pb on human health and disease. *Trace Elem Electrolytes* 40(1):1
- Zhao S, Li Z, Li K, Dai X, Xu Z, Li L, Wang H, Liu X, Li D (2024) Repairing effect of mesenchymal stem cells on lead acetate-induced testicular injury in mice. *Cell Transplant* 33:9636897231219395. <https://doi.org/10.1177/09636897231219395>
- Malik, J, Choudhary S, Mandal SC, Sarup P, Pahuja S (2022) Oxidative stress and male infertility: role of herbal drugs. *Oxidative stress and toxicity in reproductive biology and medicine: a comprehensive update on male infertility, volume II*. Springer, pp 137–159
- Haidl G, Schill WB (1991) Guidelines for drug treatment of male infertility. *Drugs* 41(1):60–68
- Martins RV, Silva AM, Duarte AP, Socorro S, Correia S, Maia CJ (2021) Natural products as protective agents for male fertility. *BioChem* 1(3):122–147
- Suleiman JB, Bakar ABA, Mohamed M (2021) Review on bee products as potential protective and therapeutic agents in male reproductive impairment. *Molecules* 26(11):3421
- Hu X, Wang Y, Chi X, Wang H, Liu Z, Ma L, Xu B (2023) Oleic acid promotes the biosynthesis of 10-hydroxy-2-decanoic acid via species-selective remodeling of TAGs in *Apis mellifera ligustica*. *Int J Mol Sci* 24(17)
- You M, Miao Z, Sienkiewicz O, Jiang X, Zhao X, Hu F (2020) 10-Hydroxydecanoic acid inhibits LPS-induced inflammation by targeting p53 in microglial cells. *Int Immunopharmacol* 84:106501
- Oršolić N, Jazvinščak Jembrek M (2024) Royal jelly: biological action and health benefits. *Int J Mol Sci* 25(11)
- Kocot J, Kiełczykowska M, Luchowska-Kocot D, Kurzepa J, Musik I (2018) Antioxidant potential of propolis, bee pollen, and royal jelly: possible medical application. *Oxid Med Cell Longev* 2018(1):7074209
- Hashem NM, Hassanein EM, Simal-Gandara J (2021) Improving reproductive performance and health of mammals using honey-bee products. *Antioxidants* 10(3):336
- Kolayli S, Sahin H, Can Z, Yildiz O, Malkoc M, Asadov A (2016) A member of complementary medicinal food: anatolian royal jellies, their chemical compositions, and antioxidant properties. *J Evid Based Complementary Altern Med* 21(4):NP43–NP48
- Chen YF, Wang K, Zhang YZ, Zheng YF, Hu FL (2016) In vitro anti-inflammatory effects of three fatty acids from royal jelly. *Mediators Inflamm* 2016(1):3583684
- Yu X, Tu X, Tao L, Daddam J, Li S, Hu F (2023) Royal jelly fatty acids: chemical composition, extraction, biological activity, and prospect. *J Functional Foods* 111:105868
- Liao Z, Alrosan M, Alu'datt MH, Tan TC (2024) 10-hydroxy decanoic acid, trans-10-hydroxy-2-decanoic acid, and sebacic acid: source, metabolism, and potential health functionalities and nutraceutical applications. *J Food Sci* 89(7):3878–3893
- Guo J, Ma B, Wang Z, Chen Y, Tian W, Dong Y (2022) Royal jelly protected against dextran-sulfate-sodium-induced colitis by improving the colonic mucosal barrier and gut microbiota. *Nutrients* 14(10):2069
- Mokaya HO, Njeru LK, Lattorff HMG (2020) African honeybee royal jelly: phytochemical contents, free radical scavenging activity, and physicochemical properties. *Food Biosci* 37:100733
- Khan I, Saeed K, Khan I (2019) Nanoparticles: properties, applications and toxicities. *Arab J Chem* 12(7):908–931
- El-Sayed A, Kamel M (2020) Advances in nanomedical applications: diagnostic, therapeutic, immunization, and vaccine production. *Environ Sci Pollut Res* 27:19200–19213
- Jha S, Rani R, Singh S (2023) Biogenic zinc oxide nanoparticles and their biomedical applications: a review. *J Inorg Organomet Polym Mater* 33(6):1437–1452

35. Ghareeb DA, Saleh SR, Seadawy MG, Nofal MS, Abdulmalek SA, Hassan SF ... El Demellawy MA (2021) Nanoparticles of ZnO/Berberine complex contract COVID-19 and respiratory co-bacterial infection in addition to elimination of hydroxychloroquine toxicity. *J Pharm Investig* 51(6): 735–757
36. Daoud NM, Aly MS, Ezzo OH, Ali NA (2021) Zinc oxide nanoparticles improve testicular steroidogenesis machinery dysfunction in benzo [α] pyrene-challenged rats. *Sci Rep* 11(1):11675
37. Pinho AR, Rebelo S, Pereira MDL (2020) The impact of zinc oxide nanoparticles on male (in) fertility. *Materials* 13(4):849
38. Khalaf A, Hassanen EI, Azouz RA, Zaki AR, Ibrahim MA, Farroh KY, Galal MK (2019) Ameliorative effect of zinc oxide nanoparticles against dermal toxicity induced by lead oxide in rats. *Int J Nanomed* 14:7729–7741. <https://doi.org/10.2147/IJN.S220572>
39. Mohamed EM, Abdel Hamid MM, Elfakharany YM (2021) Zinc oxide nanoparticles attenuate cadmium chloride induced tongue toxicity in adult male Albino rats (histological and biochemical study). *Egypt J Histol* 44(3):601–611
40. AL-Asady ZM, AL-Hamdani AH, Hussein MA (2020) Study the optical and morphology properties of zinc oxide nanoparticles. In: AIP conference proceedings 2213(1). <https://doi.org/10.1063/5.0000259>
41. Shamhari NM, Wee BS, Chin SF, Kok KY (2018) Synthesis and characterization of zinc oxide nanoparticles with small particle size distribution. *Acta Chim Slovenica* 65(3)
42. Yue B, Yang J, Wang Y, Huang C-Y, Dave R, Pfeffer R (2004) Particle encapsulation with polymers via in situ polymerization in supercritical CO₂. *Powder Technol* 146(1–2):32–45
43. Patino-Portela MC, Arciniegas-Grijalba PA, Mosquera-Sanchez LP, Sierra BEG, Munoz-Florez JE, Erazo-Castillo LA, Rodriguez-Paez JE (2021) Effect of method of synthesis on antifungal ability of ZnO nanoparticles: chemical route vs green route. *Adv Nano Res* 10(2):191–210
44. Schmickler W, Santos E (2010) *Interfacial electrochemistry*, 2nd edn. Springer Heidelberg Dordrecht London New York. <https://doi.org/10.1007/978-3-642-04937-8>
45. Sudjarwo SA, Eraiko K, Sudjarwo GW, Koerniasari (2017) Protective effects of piperine on lead acetate induced-nephrotoxicity in rats. *Iran J Basic Med Sci* 20(11): 1227–1231
46. Elgawish RAR, Abdelrazek HMA (2014) Effects of lead acetate on testicular function and caspase-3 expression with respect to the protective effect of cinnamon in albino rats. *Toxicol Rep* 1:795–801
47. Albalawi AE, Althobaiti NA, Alrdahe SS, Alhasani RH, Alaryani FS, BinMowyna MN (2021) Anti-tumor effects of queen bee acid (10-hydroxy-2-decanoic acid) alone and in combination with cyclophosphamide and its cellular mechanisms against Ehrlich solid tumor in mice. *Molecules* 26(22):7021
48. Mirzaei F, Abbasi E, Mirzaei A, Hosseini NF, Naseri N, Khodadadi I ... Majdoub N (2024) Toxicity and Hepatoprotective effects of ZnO nanoparticles on normal and high-fat diet-fed rat livers: mechanism of action. *Biol Trace Element Res*
49. Goma AA, Tohamy HG, El-Kazaz SE, Soliman MM, Shukry M, Elgazzar AM, Rashed RR (2021) Insight study on the comparison between zinc oxide nanoparticles and its bulk impact on reproductive performance, antioxidant levels, gene expression, and histopathology of testes in male rats. *Antioxidants* 10(1):41
50. Majd NE, Hajirahimi A, Tabandeh MR, Molaei R (2021) Protective effects of green and chemical zinc oxide nanoparticles on testis histology, sperm parameters, oxidative stress markers and androgen production in rats treated with cisplatin. *Cell Tissue Res* 384(2):561–575
51. Nakatsu N, Igarashi Y, Aoshi T, Hamaguchi I, Saito M, Mizukami T ... Yamada H (2017) Isoflurane is a suitable alternative to ether for anesthetizing rats prior to euthanasia for gene expression analysis. *J Toxicol Sci* 42(4): 491–497
52. Khorsandi L, Mirhoseini M, Mohamadpour M, Orazizadeh M, Khaghani S (2013) Effect of curcumin on dexamethasone-induced testicular toxicity in mice. *Pharm Biol* 51(2):206–212
53. Orazizadeh M, Khorsandi L, Hashemitabar M (2010) Toxic effects of dexamethasone on mouse testicular germ cells. *Andrologia* 42(4):247–253
54. Motoshima M, Settlege D (1978) Determination of fructose and glucose in semen: evaluation and comparison of colorimetric and enzymatic methods. *Nihon Funin Gakkai Zasshi* 23(4):454–464
55. Szkoda J, Zmudzki J (2005) Determination of lead and cadmium in biological material by graphite furnace atomic absorption spectrometry method. *Bull Vet Inst Pulawy* 49(1):89–92
56. Gur C, Kandemir O, Kandemir FM (2022) Investigation of the effects of hesperidin administration on abamectin-induced testicular toxicity in rats through oxidative stress, endoplasmic reticulum stress, inflammation, apoptosis, autophagy, and JAK2/STAT3 pathways. *Environ Toxicol* 37(3):401–412
57. Montgomery H, Dymock J (1961) The determination of nitrite in water: colorimetric method of nitric oxide assay. *Analyst* 86:414
58. Ellman GL (1959) Tissue sulfhydryl groups. *Arch Biochem Biophys* 82(1):70–77
59. Kahalerras L, Otmani I, Abdennour C (2022) Wild garlic *Allium triquetrum* L. alleviates lead acetate-induced testicular injuries in rats. *Biol Trace Element Res* 200(5):2205–2222
60. Habig WH, Pabst MJ, Jakoby WB (1974) Glutathione S-transferases: the first enzymatic step in mercapturic acid formation. *J Biol Chem* 249(22):7130–7139
61. Nandi A, Chatterjee I (1988) Assay of superoxide dismutase activity in animal tissues. *J Biosci* 13:305–315
62. Lowry O, Rosebrough N, Farr AL, Randall R (1951) Protein measurement with the Folin phenol reagent. *J Biol Chem* 193(1):265–275
63. Saleh SR, Abd-Elmegied A, Aly Madhy S, Khattab SN, Sheta E, Elnozahy FY ... Abd-Elmonem NM (2024) Brain-targeted Tet-1 peptide-PLGA nanoparticles for berberine delivery against STZ-induced Alzheimer's disease in a rat model: alleviation of hippocampal synaptic dysfunction, Tau pathology, and amyloidogenesis. *Int J Pharm* 658: 124218
64. Zhou J-R, Li L, Pan W (2007) Dietary soy and tea combinations for prevention of breast and prostate cancers by targeting metabolic syndrome elements in mice. *Am J Clin Nutr* 86(3):882S–888S
65. Bancroft JD, Layton C, Suvarna SK (2013) *Bancroft's theory and practice of histological techniques*. Elsevier Health Sciences, Churchill Livingstone: London, UK.
66. Elblehi SS, El Euony OI, El-Nahas AF (2019) Partial ameliorative effect of Moringa leaf ethanolic extract on the reproductive toxicity and the expression of steroidogenic genes induced by subchronic cadmium in male rats. *Environ Sci Pollut Res* 26:23306–23318
67. Anyanwu BO, Ezejiofor AN, Igweze ZN, Orisakwe OE (2018) Heavy metal mixture exposure and effects in developing nations: an update. *Toxics* 6(4):65
68. Wahab OA, Princely AC, Oluwadamilare AA, Oore-oluwapo DO, Blessing AO, Alfred EF (2019) Clomiphene citrate ameliorated lead acetate-induced reproductive toxicity in male Wistar rats. *JBRA Assisted Reprod* 23(4):336
69. Raeeszadeh M, Karimfar B, Amiri AA, Akbari A (2021) Protective effect of nano-vitamin C on infertility due to oxidative stress induced by lead and arsenic in male rats. *J Chem* 2021:1–12
70. Elmallah MI, Elkhadragey MF, Al-Olayan EM, Abdel Moneim AE (2017) Protective effect of *Fragaria ananassa* crude extract on cadmium-induced lipid peroxidation, antioxidant enzymes suppression, and apoptosis in rat testes. *Int J Mol Sci* 18(5):957

71. Mabrouk A, Ben Cheikh H (2016) Thymoquinone supplementation ameliorates lead-induced testis function impairment in adult rats. *Toxicol Ind Health* 32(6):1114–1121
72. Massányi P, Massányi M, Madeddu R, Stawarz R, Lukáč N (2020) Effects of cadmium, lead, and mercury on the structure and function of reproductive organs. *Toxics* 8(4):94
73. Dkhil MA, Moneim AEA, Al-Quraishi S (2016) *Indigofera oblongifolia* ameliorates lead acetate-induced testicular oxidative damage and apoptosis in a rat model. *Biol Trace Elem Res* 173:354–361
74. Lu T, Ling C, Hu M, Meng X, Deng Y, An H ... Song G (2021) Effect of nano-titanium dioxide on blood-testis barrier and MAPK signaling pathway in male mice. *Biol Trace Element Res* 199: 2961–2971
75. Sharma A, Mollier J, Brocklesby RW, Caves C, Jayasena CN, Minhas S (2020) Endocrine-disrupting chemicals and male reproductive health. *Reprod Med Biol* 19(3):243–253
76. Flora G, Gupta D, Tiwari A (2012) Toxicity of lead: a review with recent updates. *Interdiscip Toxicol* 5(2):47–58
77. Ali SA, Al-Derawi KH, Almansour N, Monsour A (2018) Testicular toxic effect of lead acetate on adult male rats and the potential protective role of alcoholic extract of ginseng (histological, histomorphometrical and physiological). *Scientific Journal of Medical Research* 2:87–92. <https://doi.org/10.37623/SJMR.2018.2607>
78. Abu-Khudir R, Almutairi HH, Abd El-Rahman SS, El-Said KS (2023) The palliative and antioxidant effects of hesperidin against lead-acetate-induced testicular injury in male Wistar rats. *Biomedicines* 11(9):2390
79. Xie Y, He Y, Irwin PL, Jin T, Shi X (2011) Antibacterial activity and mechanism of action of zinc oxide nanoparticles against *Campylobacter jejuni*. *Appl Environ Microbiol* 77(7):2325–2331
80. Keerthana P, Vijayakumar S, Vidhya E, Punitha V, Nilavukkarasi M, Praseetha P (2021) Biogenesis of ZnO nanoparticles for revolutionizing agriculture: a step towards anti-infection and growth promotion in plants. *Ind Crops Prod* 170:113762
81. Rasmussen JW, Martinez E, Louka P, Wingett DG (2010) Zinc oxide nanoparticles for selective destruction of tumor cells and potential for drug delivery applications. *Expert Opin Drug Deliv* 7(9):1063–1077
82. Abedin SN, Baruah A, Baruah KK, Bora A, Dutta DJ, Kadirvel G ... Deori S (2023) Zinc oxide and selenium nanoparticles can improve semen quality and heat shock protein expression in cryopreserved goat (*Capra hircus*) spermatozoa. *J Trace Elem Med Biol* 80: 127296
83. Ahmed DH, El-Beih NM, El-Hussieny EA, El-Sayed WM (2024) Zinc oxide nanoparticles induced testicular toxicity through inflammation and reducing testosterone and cell viability in adult male rats. *Biol Trace Element Res* 1–15. <https://doi.org/10.1007/s12011-024-04330-1>
84. Abdelnour SA, Abd El-Hack ME, Alagawany M, Taha AE, Elnesr SS, Abd Elmonem OM, Swelum AA (2020) Useful impacts of royal jelly on reproductive sides, fertility rate and sperm traits of animals. *J Anim Physiol Anim Nutr* 104(6):1798–1808
85. El Helew EA, Hamed WS, Moustafa AM, Sakkara ZA (2024) Structural changes in testes of Streptozotocin induced diabetic rats and possible protective effect of royal jelly: light and electron microscopic study. *Ultrastruct Pathol* 48(1):1–15
86. Safaei Pourzamani M, Oryan S, Yaghmaei P, Jalili C, Ghanbari A (2022) Royal jelly alleviates side effects of doxorubicin on male reproductive system: a mouse model simulated human chemotherapy cycles. *Res J Pharmacogn* 9(1):77–87
87. Afifi M, Almaghrabi OA, Kadasa NM (2015) Ameliorative effect of zinc oxide nanoparticles on antioxidants and sperm characteristics in streptozotocin-induced diabetic rat testes. *Biomed Res Int* 2015:153573
88. Takeshima T, Usui K, Mori K, Asai T, Yasuda K, Kuroda S, Yumura Y (2021) Oxidative stress and male infertility. *Reprod Med Biol* 20(1):41–52
89. Kurutas EB (2015) The importance of antioxidants which play the role in cellular response against oxidative/nitrosative stress: current state. *Nutr J* 15(1):1–22
90. Baskaran S, Finelli R, Agarwal A, Henkel R (2021) Reactive oxygen species in male reproduction: a boon or a bane? *Andrologia* 53(1):e13577
91. Assi MA, Hezmee MNM, Sabri MYM, Rajion MA (2016) The detrimental effects of lead on human and animal health. *Veterinary world* 9(6):660
92. Obafemi TO, Onasanya A, Adeoye A, Falode JA, Daniel DJ, Irefo EF ... Omiyale BO (2019) Protective effect of methanolic and flavonoid-rich leaf extracts of *Synsepalum dulcificum* (Danielli) on lead-acetate-induced toxicity in Wistar albino rats. *J App Pharm Sci* 9(5): 065-072
93. Azad F, Nejati V, Shalazar-Jalali A, Najafi G, Rahmani F (2019) Antioxidant and anti-apoptotic effects of royal jelly against nicotine-induced testicular injury in mice. *Environ Toxicol* 34(6):708–718
94. Prasad AS, Bao B (2019) Molecular mechanisms of zinc as a pro-antioxidant mediator: clinical therapeutic implications. *Antioxidants (Basel)* 8(6)
95. Ghorbani A, Moeini MM, Soury M, Hajarian H, Kachuee R (2024) Effect of dietary zinc, selenium and their combination on antioxidant parameters in serum and Semen of Sanjabi mature rams. *J Trace Elem Min* 8:100118
96. Mansouri A, Reiner Ž, Ruscica M, Tedeschi-Reiner E, Radbakhsh S, Bagheri Ekta M, Sahebkar A (2022) Antioxidant effects of statins by modulating Nrf2 and Nrf2/HO-1 signaling in different diseases. *J Clin Med* 11(5):1313
97. Yang K, Li W-F, Yu J-F, Yi C, Huang W-F (2017) Diosmetin protects against ischemia/reperfusion-induced acute kidney injury in mice. *J Surg Res* 214:69–78
98. Awadalla A, Hamam ET, El-Senduny FF, Omar NM, Mahdi MR, Barakat N ... Khirallah SM (2022) Zinc oxide nanoparticles and spironolactone-enhanced Nrf2/HO-1 pathway and inhibited Wnt/ β -catenin pathway in adenine-induced nephrotoxicity in rats. *Redox Rep* 27(1): 249-258
99. Hassan E, Kahilo K, Kamal T, El-Neweshy M, Hassan M (2019) Protective effect of diallyl sulfide against lead-mediated oxidative damage, apoptosis and down-regulation of CYP19 gene expression in rat testes. *Life Sci* 226:193–201
100. Wang Y, Fang J, Huang S, Chen L, Fan G, Wang C (2013) The chronic effects of low lead level on the expressions of Nrf2 and Mrp1 of the testes in the rats. *Environ Toxicol Pharmacol* 35(1):109–116
101. Almeer RS, Soliman D, Kassab RB, AlBasher GI, Alarifi S, Alkahtani S ... Abdel Moneim AE (2018) Royal jelly abrogates cadmium-induced oxidative challenge in mouse testes: involvement of the Nrf2 pathway. *Int J Mol Sci* 19(12): 3979
102. Ommati MM, Ahmadi HN, Sabouri S, Retana-Marquez S, Abdoli N, Rashno S ... Rezaei M (2022) Glycine protects the male reproductive system against lead toxicity via alleviating oxidative stress, preventing sperm mitochondrial impairment, improving kinematics of sperm, and blunting the downregulation of enzymes involved in the steroidogenesis. *Environ Toxicol* 37(12): 2990–3006
103. Aitken RJ, Drevet JR, Moazamian A, Gharagozloo P (2022) Male infertility and oxidative stress: a focus on the underlying mechanisms. *Antioxidants* 11(2):306
104. Gandhi J, Hernandez RJ, Chen A, Smith NL, Sheynkin YR, Joshi G, Khan SA (2017) Impaired hypothalamic-pituitary-testicular axis activity, spermatogenesis, and sperm function

- promote infertility in males with lead poisoning. *Zygote* 25(2):103–110
105. Nsonwu-Anyanwu AC, Ekong ER, Offor SJ, Awusha OF, Orji OC, Umoh EI ... Usoro CAO (2019) Heavy metals, biomarkers of oxidative stress and changes in sperm function: a case-control study. *Int J Reprod Biomed* 17(3): 163
 106. Rao F, Zhai Y, Sun F (2016) Punicalagin mollifies lead acetate-induced oxidative imbalance in male reproductive system. *Int J Mol Sci* 17(8)
 107. Offor SJ, Mbagwu HO, Orisakwe OE (2019) Improvement of lead acetate-induced testicular injury and sperm quality deterioration by *Solanum anomalum* thonn. ex. *schumach* fruit extracts in Albino rats. *J Family Reprod Health* 13(2):98–108
 108. Mobasher MA, Alsirhani AM, Alwaili MA, Baakdah F, Eid TM, Alshambari FA ... El-Said KS (2024) *Annona squamosa* fruit extract ameliorates lead acetate-induced testicular injury by modulating JAK-1/STAT-3/SOCS-1 signaling in male rats. *Int J Mol Sci* 25(10): 5562
 109. Çavuşoğlu K, Yapar K, Yalçın E (2009) Royal jelly (honey bee) is a potential antioxidant against cadmium-induced genotoxicity and oxidative stress in albino mice. *J Med Food* 12(6):1286–1292
 110. Karimi-Sabet MJ, Khodaei-Motlagh M, Masoudi R, Sharafi M (2024) Zinc oxide nanoparticles preserve the quality and fertility potential of rooster sperm during the cryopreservation process. *Reprod Domest Anim* 59(4):e14568
 111. Hozyen HF, Shamy AAE, Fattah EMAE, Sakr AM (2023) Facile fabrication of zinc oxide nanoparticles for enhanced buffalo sperm parameters during cryopreservation. *J Trace Elem Min* 4:100058
 112. Saleh SR, Attia R, Ghareeb DA (2018) The ameliorating effect of berberine-rich fraction against gossypol-induced testicular inflammation and oxidative stress. *Oxid Med Cell Longev* 2018:1056173
 113. Witkowska D, Słowik J, Chilicka K (2021) Heavy metals and human health: possible exposure pathways and the competition for protein binding sites. *Molecules* 26(19):6060
 114. Barbagallo F, La Vignera S, Cannarella R, Crafa A, Calogero AE, Condorelli RA (2021) The relationship between seminal fluid hyperviscosity and oxidative stress: a systematic review. *Antioxidants* 10(3):356
 115. Kandemir FM, Caglayan C, Aksu EH, Yildirim S, Kucukler S, Gur C, Eser G (2020) Protective effect of rutin on mercuric chloride-induced reproductive damage in male rats. *Andrologia* 52(3):e13524
 116. Jomova K, Raptova R, Alomar SY, Alwasel SH, Nepovimova E, Kuca K, Valko M (2023) Reactive oxygen species, toxicity, oxidative stress, and antioxidants: chronic diseases and aging. *Arch Toxicol* 97(10):2499–2574
 117. Mittal M, Siddiqui MR, Tran KA, Reddy SP, Malik AB (2014) Reactive oxygen species in inflammation and tissue injury. *Antioxidants Redox Signal* 20(7):1126–1167. <https://doi.org/10.1089/ars.2012.5149>
 118. Hu X, Liu Z, Lu Y, Chi X, Han K, Wang H ... Xu B (2022) Glucose metabolism enhancement by 10-hydroxy-2-decenoic acid via the PI3K/AKT signaling pathway in high-fat-diet/streptozotocin induced type 2 diabetic mice. *Food Funct* 13(19): 9931–9946
 119. Olesen J (2008) The role of nitric oxide (NO) in migraine, tension-type headache and cluster headache. *Pharmacol Ther* 120(2):157–171
 120. Li Y-J, Shimizu T, Hirata Y, Inagaki H, Takizawa H, Azuma A ... Sunazuka T (2013) EM, EM703 inhibit NF-κB activation induced by oxidative stress from diesel exhaust particle in human bronchial epithelial cells: importance in IL-8 transcription. *Pulm Pharmacol Ther* 26(3): 318–324
 121. Anilkumar S, Wright-Jin E (2024) NF-κB as an inducible regulator of inflammation in the central nervous system. *Cells* 13(6):485
 122. Huang H, Li X, Wang Z, Lin X, Tian Y, Zhao Q, Zheng P (2020) Anti-inflammatory effect of selenium on lead-induced testicular inflammation by inhibiting NLRP3 inflammasome activation in chickens. *Theriogenology* 155:139–149
 123. Besong EE, Ashonibare PJ, Akhigbe TM, Obimma JN, Akhigbe RE (2024) Sodium acetate abates lead-induced sexual dysfunction by upregulating testosterone-dependent eNOS/NO/cGMP signaling and activating Nrf2/HO-1 in male Wistar rat. *Naunyn Schmiedebergs Arch Pharmacol* 397(2):1233–1243
 124. Ileriturk M, Benzer F, Aksu EH, Yildirim S, Kandemir FM, Dogan T ... Genc A (2021) Chrysin protects against testicular toxicity caused by lead acetate in rats with its antioxidant, anti-inflammatory, and antiapoptotic properties. *J Food Biochem* 45(2): e13593
 125. Tuncer SÇ, Akarsu SA, Küçükler S, Gür C, Kandemir FM (2023) Effects of sinapic acid on lead acetate-induced oxidative stress, apoptosis and inflammation in testicular tissue. *Environ Toxicol* 38(11):2656–2667
 126. Bidanchi RM, Lalrindika L, Khushboo M, Bhanushree B, Dinata R, Das M ... Saeed-Ahmed L (2022) Antioxidative, anti-inflammatory and anti-apoptotic action of ellagic acid against lead acetate induced testicular and hepato-renal oxidative damages and pathophysiological changes in male Long Evans rats. *Environ Poll* 302: 119048
 127. Yang Y-C, Chou W-M, Widowati DA, Lin I-P, Peng C-C (2018) 10-hydroxy-2-decenoic acid of royal jelly exhibits bactericidal and anti-inflammatory activity in human colon cancer cells. *BMC Complement Altern Med* 18:1–7
 128. Kim M-H (2016) Biological effects of zinc oxide nanoparticles on inflammation. *Tang [Humanitas Medicine]* 6(4):22–27. <https://doi.org/10.5667/tang.2016.0013>
 129. Goma AA, Salama AR, Tohamy HG, Rashed RR, Shukry M, El-Kazaz SE (2024) Examining the influence of zinc oxide nanoparticles and bulk zinc oxide on rat brain functions: a comprehensive neurobehavioral, antioxidant, gene expression, and histopathological investigation. *Biol Trace Elem Res* 202:4654–4673. <https://doi.org/10.1007/s12011-023-04043-x>
 130. Anjum MR, Madhu P, Reddy KP, Reddy PS (2017) The protective effects of zinc in lead-induced testicular and epididymal toxicity in Wistar rats. *Toxicol Ind Health* 33(3):265–276
 131. Owumi SE, Arunsi UO, Otunla MT, Oluwasuji IO (2023) Exposure to lead and dietary furan intake aggravates hypothalamus-pituitary-testicular axis toxicity in chronic experimental rats. *J Biomed Res* 37(2):100
 132. Sokol RZ, Madding CE, Swerdloff RS (1985) Lead toxicity and the hypothalamic-pituitary-testicular axis. *Biol Reprod* 33(3):722–728
 133. Singh N, Kumar A, Gupta VK, Sharma B (2018) Biochemical and molecular bases of lead-induced toxicity in mammalian systems and possible mitigations. *Chem Res Toxicol* 31(10):1009–1021
 134. Darbandi M, Darbandi S, Agarwal A, Sengupta P, Durairajanayagam D, Henkel R, Sadeghi MR (2018) Reactive oxygen species and male reproductive hormones. *Reprod Biol Endocrinol* 16(1):1–14
 135. Baltaci AK, Mogulkoc R, Baltaci SB (2019) Review: the role of zinc in the endocrine system. *Pak J Pharm Sci* 32(1):231–239
 136. Mozaffari Z, Parivar K, Roodbari NH, Irani S (2020) The impact of zinc oxide nanoparticle on LH, FSH, and testosterone hormones in mature male NMRI rats. *J Pharm Res Int* 32(4):30–37
 137. Selvakumar K, Krishnamoorthy G, Venkataraman P, Arunakaran J (2013) Reactive oxygen species induced oxidative stress,

- neuronal apoptosis and alternative death pathways. *Adv Biosci Biotechnol* 4(01):14–21
138. Şimşek H, Akaras N, Gür C, Küçükler S, Kandemir FM (2023) Beneficial effects of Chrysin on Cadmium-induced nephrotoxicity in rats: modulating the levels of Nrf2/HO-1, RAGE/NLRP3, and Caspase-3/Bax/Bcl-2 signaling pathways. *Gene* 875:147502
139. Abdrabou MI, Elleithy EM, Yasin NA, Shaheen YM, Galal M (2019) Ameliorative effects of *Spirulina maxima* and *Allium sativum* on lead acetate-induced testicular injury in male albino rats with respect to caspase-3 gene expression. *Acta Histochem* 121(2):198–206
140. AL-Megrin WA, Alomar S, Alkhuriji AF, Metwally DM, Mohamed SK, Kassab RB ... El-Khadragy MF (2020) Luteolin protects against testicular injury induced by lead acetate by activating the Nrf2/HO-1 pathway. *IUBMB life* 72(8):1787–1798
141. Karadeniz A, Simsek N, Karakus E, Yildirim S, Kara A, Can I ... Turkeli M (2011) Royal jelly modulates oxidative stress and apoptosis in liver and kidneys of rats treated with cisplatin. *Oxid Med Cell Longev* 2011: 981793
142. Hamza RZ, Al-Eisa RA, El-Shenawy NS (2022) Possible ameliorative effects of the royal jelly on hepatotoxicity and oxidative stress induced by molybdenum nanoparticles and/or cadmium chloride in male rats. *Biology* 11(3):450
143. Zhang Y, Geng S, Di Y, Sun Y, Liu Y, Li J, Zhang L (2022) 10-Hydroxy-trans-2-decenoic acid, a new potential feed additive for broiler chickens to improve growth performance. *Animals* 12(14):1846

Publisher's Note Springer Nature remains neutral with regard to jurisdictional claims in published maps and institutional affiliations.